Neutron scattering as a tool for atomic and magnetic structural characterization

Anatoly M. Balagurov

Frank Laboratory of Neutron Physics, JINR, Dubna, Russia

1 nm = 10^{-6} mm = 10^{-9} m = 10 Å

- **Elastic neutron scattering (diffraction)**
- **What kind of data can be obtained by neutron diffraction**

  Scattering as Fourier transform. Length scale. Overcoming of diffraction limit. Resolution in direct and reciprocal space. Phase problem.
- **Experimental technique: λ_0 and TOF neutron diffractometers**

  Steady state and pulsed research neutron sources. λ_0 *vs*. TOF modes of neutron diffraction. New possibilities of high-intensity and high-resolution neutron diffraction.
- **Basic goals of neutron structural analysis**

  Single crystals. Powders. Magnetic structure. Local distortions. Crystal microstructure. Real-Time studies. Artificial and natural nanostructures. Neutrons and electrochemistry.
- **What's in World, Russia, Dubna?**

Neutron scattering (нейтронография)

Neutron scattering in condensed matter is used for studying its structure and dynamics at atomic (molecular) level. For this low energy neutrons are used: typical energy and wavelength are about of 0.02 eV and 2 Å.

Main parts:

- atomic structure
- magnetic structure
- atomic and magnetic dynamics

Main techniques:

- diffraction
- small angle scattering
- reflectometry
- inelastic scattering

"Нейтроны и твердое тело" под редакцией Р.П.Озерова (трехтомник):
т. 1 "Структурная нейтронография", т. 2 "Нейтронография магнетиков"
т. 3 "Нейтронная спектроскопия"

Interaction of slow neutrons with matter

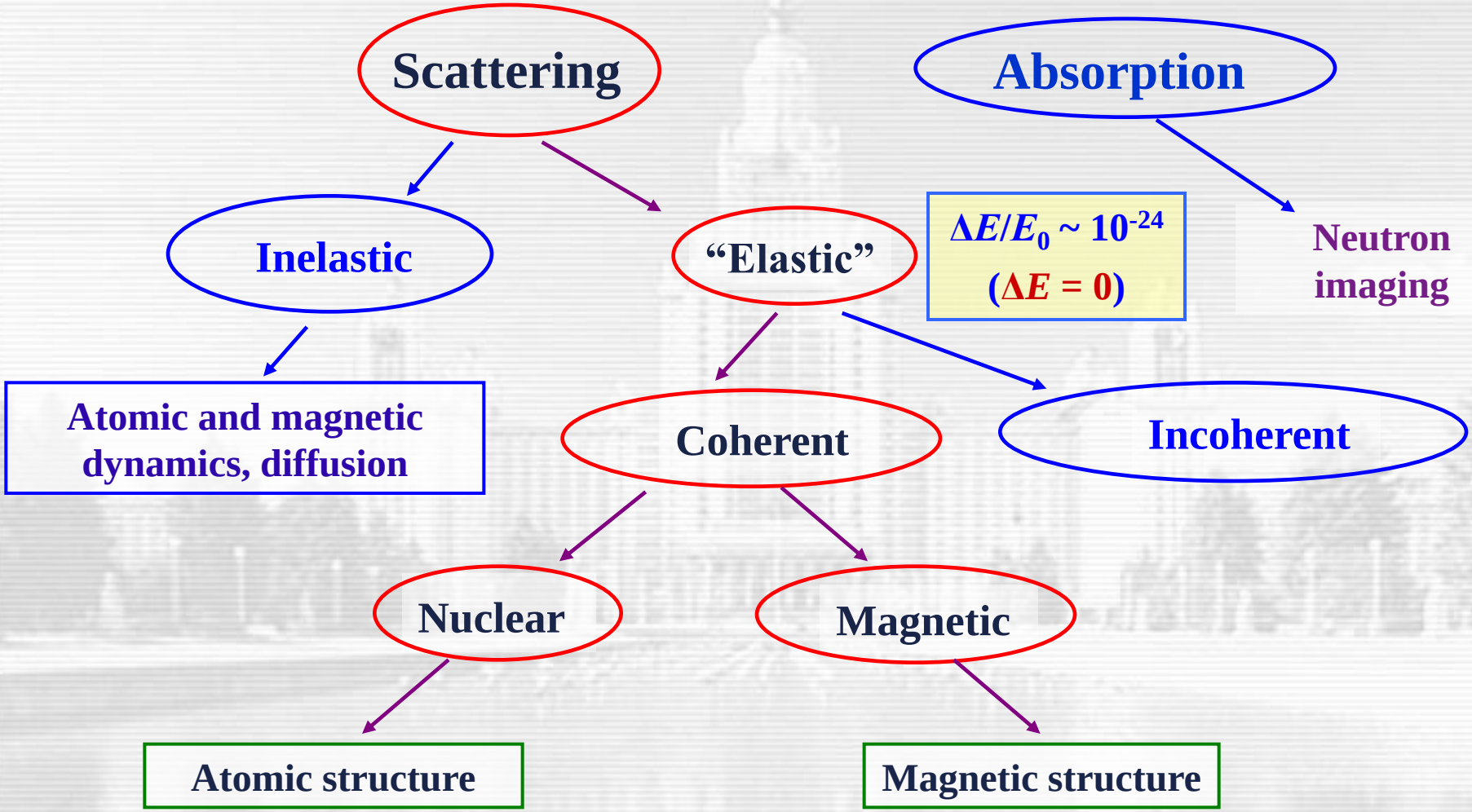

All types of interactions are used in particular experiments!

The scattering process is quite different for neutrons, X-rays and electrons

For low energy neutrons (*b* is coherent scattering length of a nuclei):

1) ***b*** **does not depend on κ (large Q-range, thermal factors)**

2) **there is no regularity in *b* dependence on atomic number (light elements visibility is good)**

3) **there is no regularity in *b* dependence on nuclear mass (isotope contrasting)**

$b_H = -0.37$ $\quad$ $b_{Fe\text{-}56} = 1.01$

$b_D = 0.67$ $\quad$ $b_{Fe\text{-}57} = 0.23$

4) ***b*** **can be < 0 ("zero" matrix)**

5) **strong magnetic scattering (magnetic structure)**

6) **small absorption (high penetration depth)**

Neutrons, Light, X-Rays, Electrons

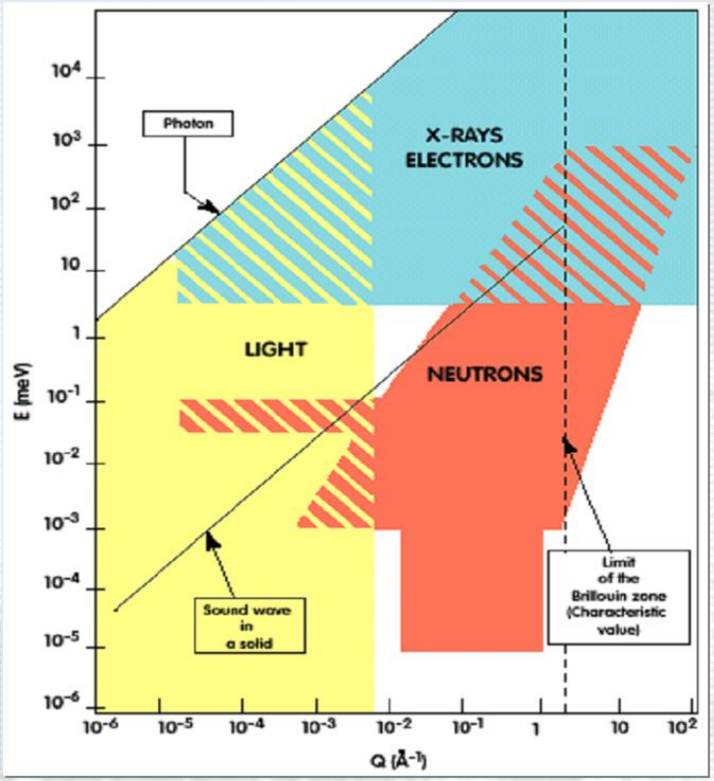

(E, Q) domains for photons and slow neutrons

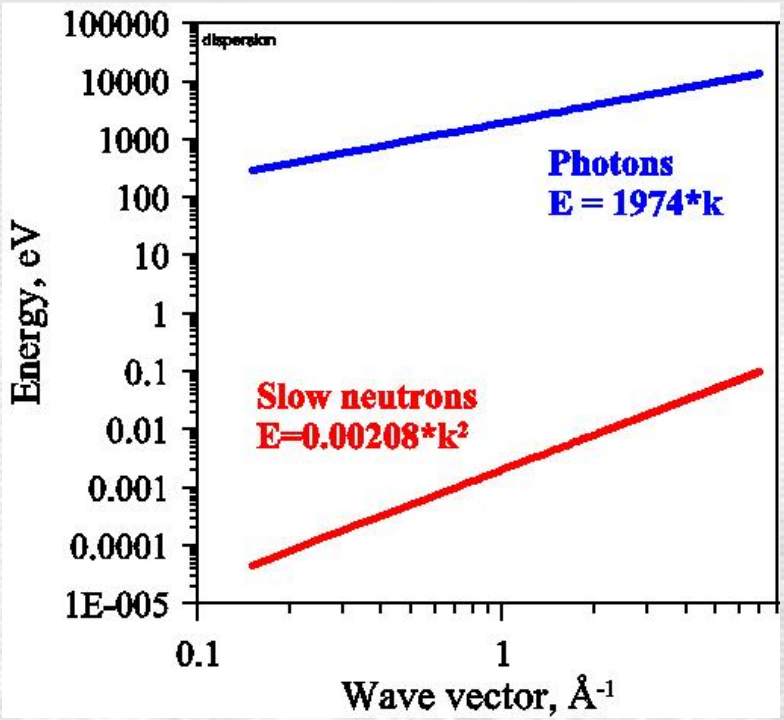

Dispersion relations for photons and neutrons

$$I(q, \omega) \sim \iint e^{i(qr - \omega t)} G(r, t) dr dt$$

(L. van Hove, 1954 г.)

$$l \sim 2\pi/q, \quad \tau \sim 2\pi/\omega$$

$$\Delta l = (0.1 - 6 \cdot 10^3)\ \text{Å}$$

Diffraction on crystal:

Elastic scattering under constraints of two (at least) conditions:

- **periodicity of scattering centers (long-range order → crystal)**
- **coherence of scattered waves (no randomness)**

Diffraction pattern is peak-like intensity distribution, which contrast depends on degree of realization of these conditions!

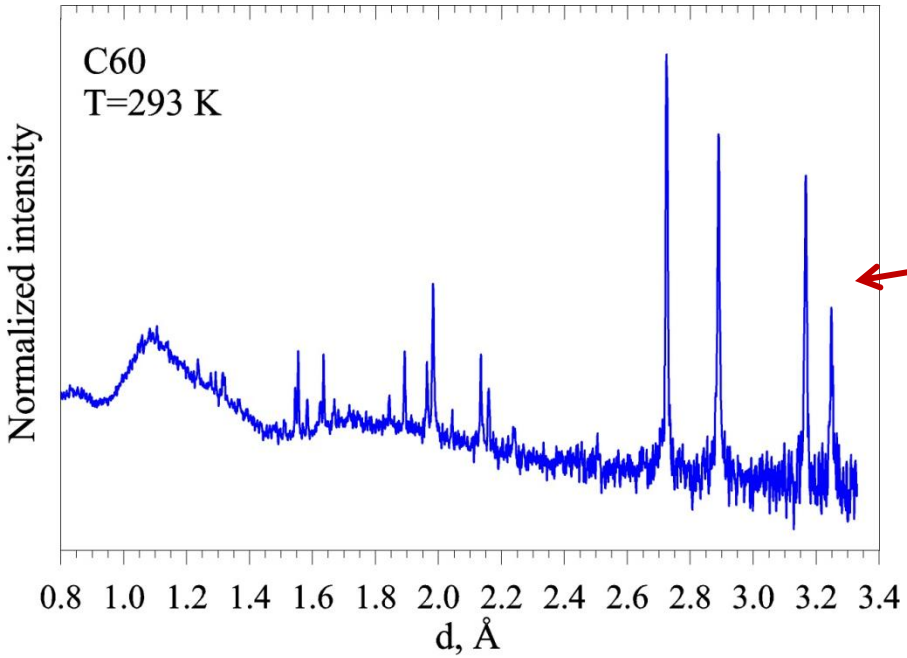

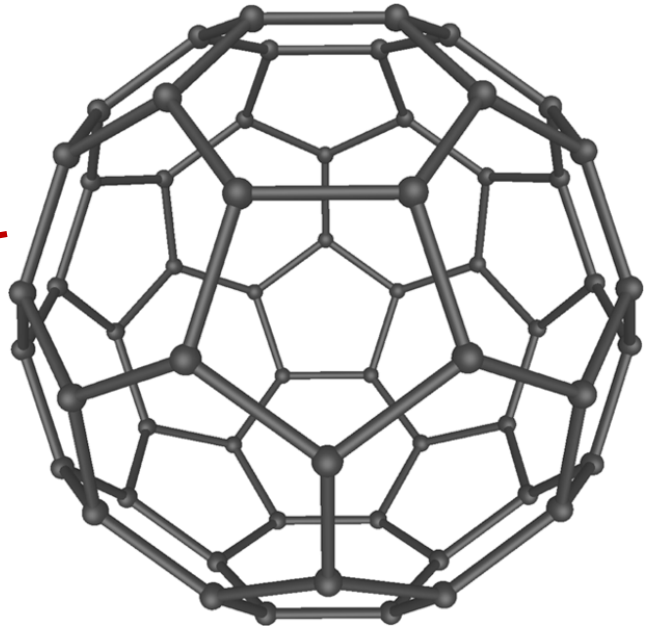

Buckminsterfullerene C60

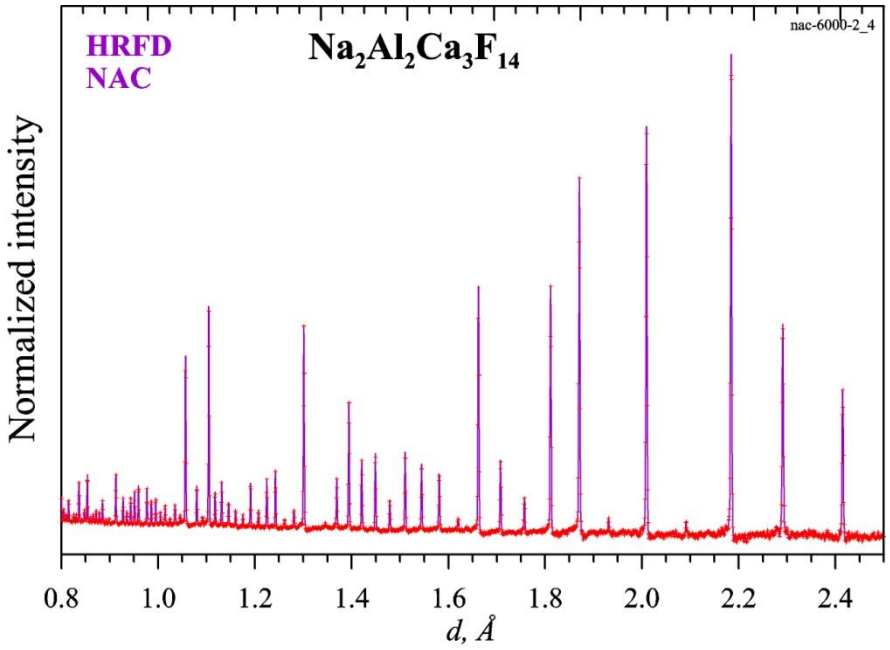

Local disorder in the C60 crystal leads to disappearance of diffraction lines at small d_{hkl} and to appearance of strong modulated incoherent scattering.
Contrary, the atomic structure of the $Na_2Al_2Ca_3F_{14}$ crystal is well ordered.

Neutron diffraction is a quantum process!

Neutron is a quantum particle!

In accordance with wave–particle duality principle neutron has mass, momentum, wavelength

For free neutron:

$\Psi(x) \sim \exp(ikx)$, $\mathbf{p} = \hbar\mathbf{k}$, $\mathbf{k}$ is wave vector,

$k = 2\pi/\lambda$, λ is de Broglie wavelength

To analyze neutron scattering on crystal we need to solve Schrödinger equation:

$$-(\hbar^2/2m)\Delta\Psi(\mathbf{r}, t) + V(\mathbf{r})\Psi(\mathbf{r}, t) = i\hbar\partial\Psi(\mathbf{r}, t)/\partial t$$

or $$-(\hbar^2/2m)\Delta\Psi(\mathbf{r}) + V(\mathbf{r})\Psi(\mathbf{r}) = E\Psi(\mathbf{r})$$

$\sigma(\boldsymbol{\kappa})=(2\pi)^3/V_c^2\cdot|F(\mathbf{H})|^2\cdot\delta(\boldsymbol{\kappa}-2\pi\mathbf{H})$ – **differential scattering cross-section**

Louis de Broglie
15.08.1892, France
19.03.1987, France

Erwin Schrödinger
12.08.1887, Austria
04.01.1961, Austria

Scattering on the aggregate of atoms

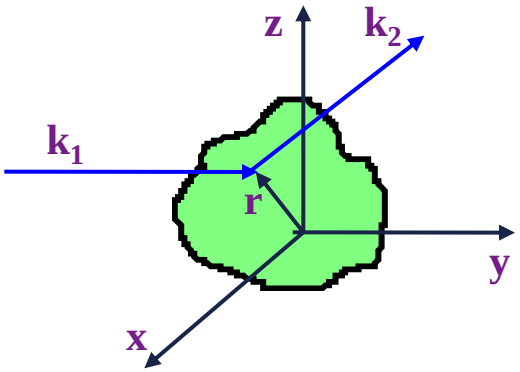

Huygens–Fresnel principle

$$f \sim \exp(i\mathbf{k}_2\mathbf{R}) \cdot \sum_j b(\mathbf{r}_j) \cdot \exp\{i(\mathbf{k}_2 - \mathbf{k}_1)\mathbf{r}_j\}$$

If an object is organized as an infinite crystal:

$$\mathbf{f \sim F \cdot \delta(q - 2\pi H)}, \quad F = \sum_j b(\boldsymbol{r}_j) \cdot \exp(i\mathbf{q}\boldsymbol{r}_j)$$

H is a vector in reciprocal lattice,

$\mathbf{q} = \mathbf{k}_2 - \mathbf{k}_1 = 2\pi\mathbf{H} \rightarrow$ $\mathbf{2}\boldsymbol{d}\ \mathbf{\sin\theta = \lambda}$

which is Bragg equation

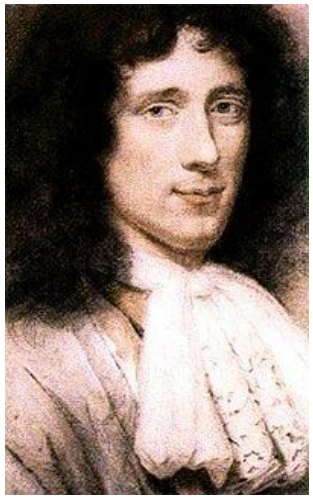

йгенс
(Christiaan Huygens)
14.04.1629 – 8.07.1695
Holland

ль
(Augustin-Jean Fresnel)
10.05.1788 – 14.07.1827
France

Elastic scattering is Fourier transformation of a structure

Intensity

$$I(q) \sim |f(q)|^2$$

Amplitude

$$I(q) \sim \int e^{iqr}\, G(r)dr$$

$$f(q) \sim \int e^{iqr}\, b(r)dr$$

$$G(r) \sim \int e^{-iqr}\, I(q)dq \quad \longleftrightarrow \quad b(r) \sim \int e^{-iqr}\, f(q)dq$$

Pair correlation function

Scattering density

$$G(r) = \int b(u)\, b(u + r)\, du$$

b(*r*) / G(*r*) - object ⟷ **f(q) / I(q) - image**

Crystal space ⟷ **Reciprocal space**

These formulae are valid for objects of any nature, any configuration of scattering centers, any type of elastic scattering, any radiation!

Crystal space to reciprocal space transformation

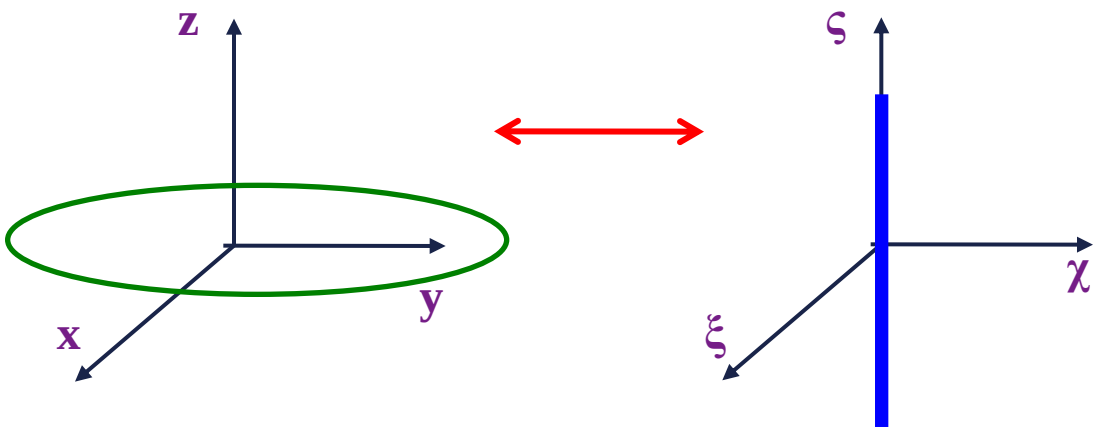

"Tablet" "Rod"

Image size along a_j is inversely proportional to object size along b_j

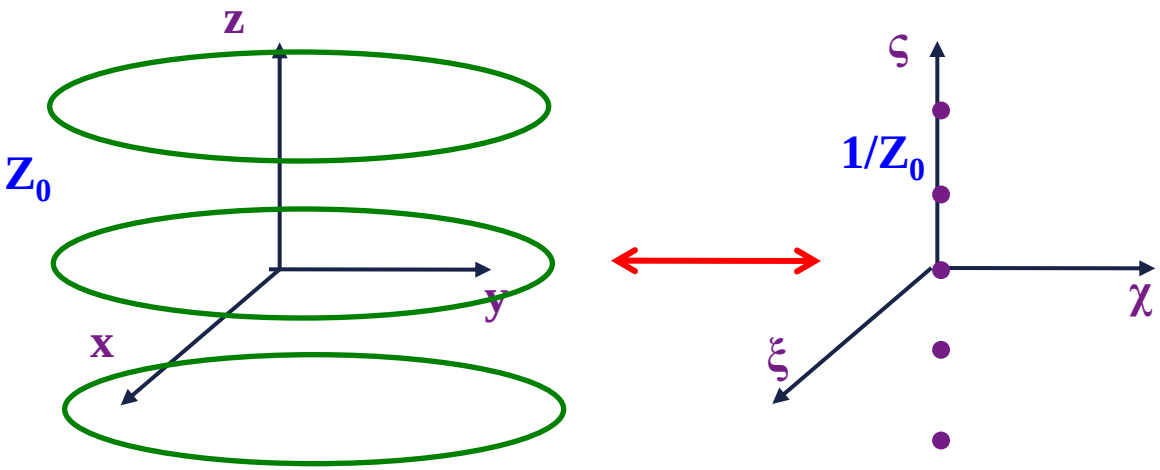

"Tablets" with period $T = Z_0$ "Points" with period $T = 1/Z_0$

Object periodicity along a_j results in image periodicity along b_j

Overcoming of the diffraction limit

$$b(r) \sim \int_0^{\infty} e^{-iqr} f(q)dq \longrightarrow b(r) \sim \int_0^{Q} e^{-iqr} f(q)dq, \quad Q = q_{max}$$

$$l_c \approx 2\pi/Q \geq \lambda_{min}/2 - \text{diffraction limit}$$

As a rule,	for diffraction	$\lambda_{min} \approx 1$ Å, i.e. $l_c \approx 0.5$ Å,
	for SANS	$Q \approx 0.5$ Å^{-1}, i.e. $l_c \approx 20$ Å.

Precision of interatomic lengths	$\sigma \sim 0.002$ Å,
Precision of lattice parameters	$\sigma \sim 0.0001$ Å,
Geometrical parameters of globular molecule	$\sigma \sim 0.2$ Å.

Diffraction limit can be overcome owing to:

- periodicity of crystal structure,
- parametric model

Neutron sources for condensed matter studies

I. Continuous neutron sources

W = 2 – 100 MW
Const in time

Region	Operational RRs
Africa	9
Americas	66
Asia/Pacific	59
Europe (with Russia)	100

234/50/15

FRM II, Germany
ANSTO, Australia
CARR, China
PIK, Russia

II. Pulsed neutron sources

W = 0.1 – 5 MW
Pulsed in time

Region	Operational PSs
Africa	0
Americas	2
Asia/Pacific	1
Europe (with Russia)	2

5

ISIS, UK
LANSCE, USA
SNS, USA
J-SNS, Japan
IBR-2M, Russia

ESS, Europe
LANSCE (new)
Ch-SNS, China
IN-06, Russia

Diffraction at steady state and at pulsed neutron sources

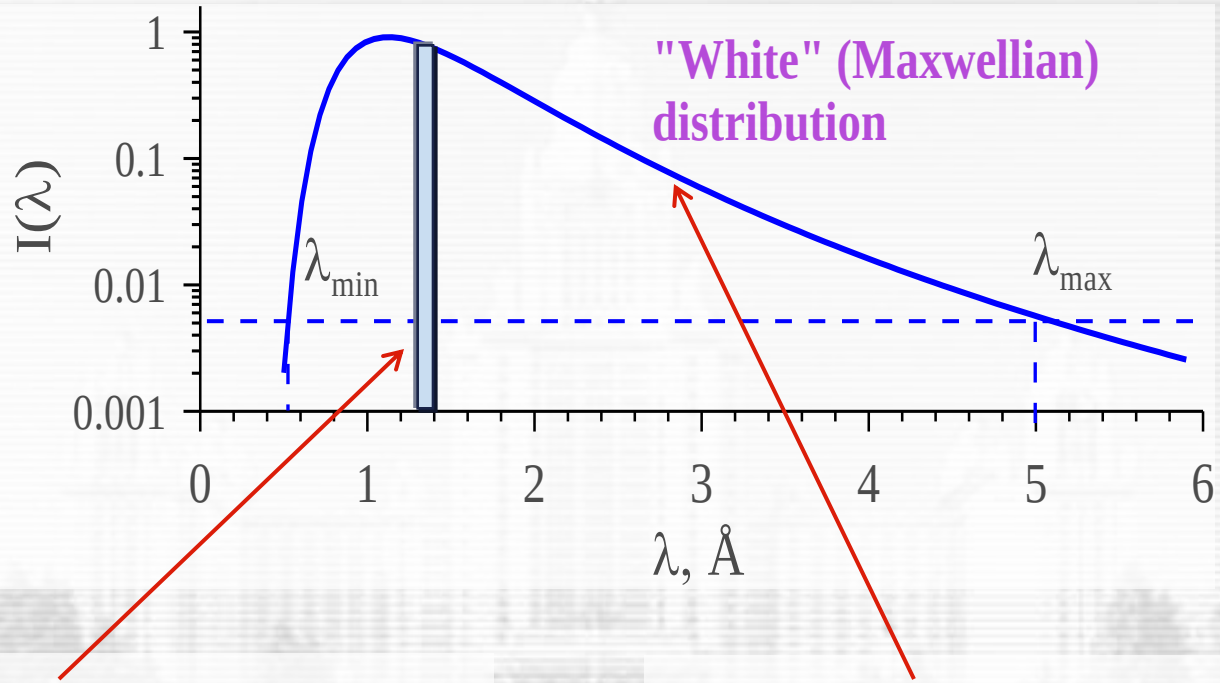

Monochromatic beam:

λ = const ≈ 1.4 Å, $\Delta\lambda/\lambda \approx 0.01$

W = (10 – 100) MW = const

Scanning in wide angular range

(λ_0-diffractometer)

"White" beam:

$\lambda_{min} \le \lambda \le \lambda_{max}$, $\Delta\lambda \approx 5 – 15$ Å

W = (0.01 – 2) MW, regular pulses

Scanning over time-of-flight (TOF), fixed geometry is possible

(TOF-diffractometer)

Neutron TOF-diffractometer

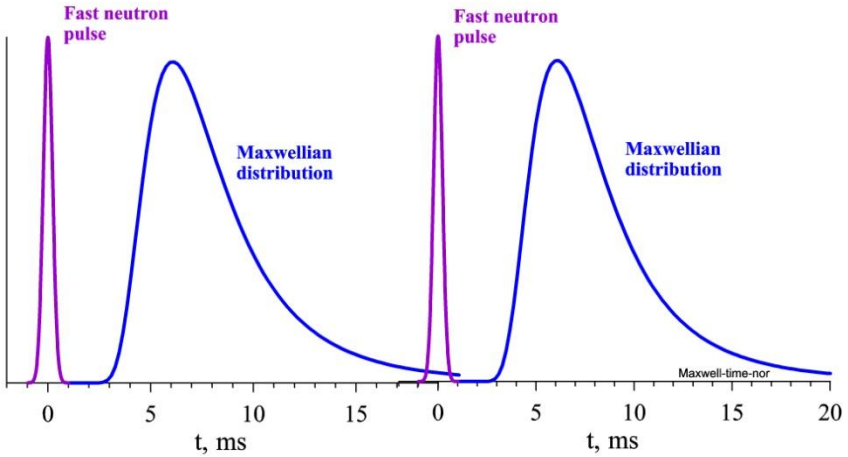

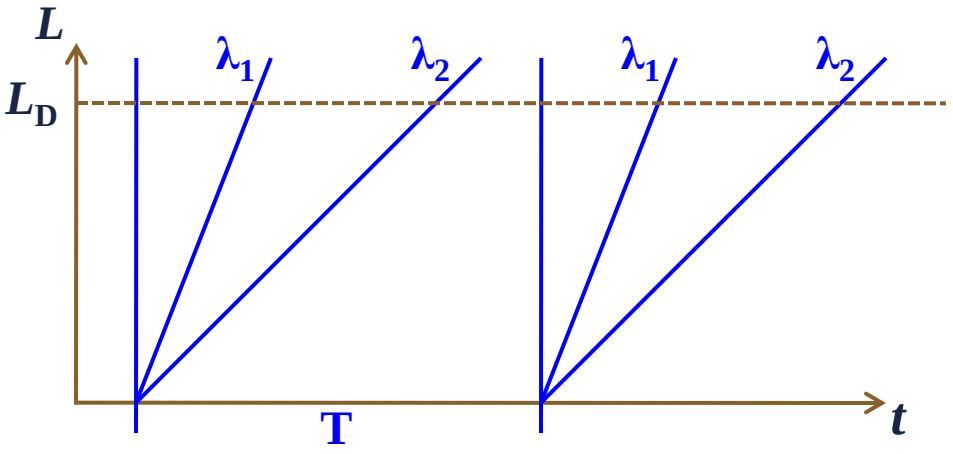

Pulses:

$\Delta T = (20 - 400)\ \mu s$

$T = (10 - 200)\ ms$

$t = 252.778 \cdot L \cdot \lambda$

$t_1 \le t \le t_2$

$\lambda_1 \le \lambda \le \lambda_2$

$2d\sin\theta_0 = \lambda$

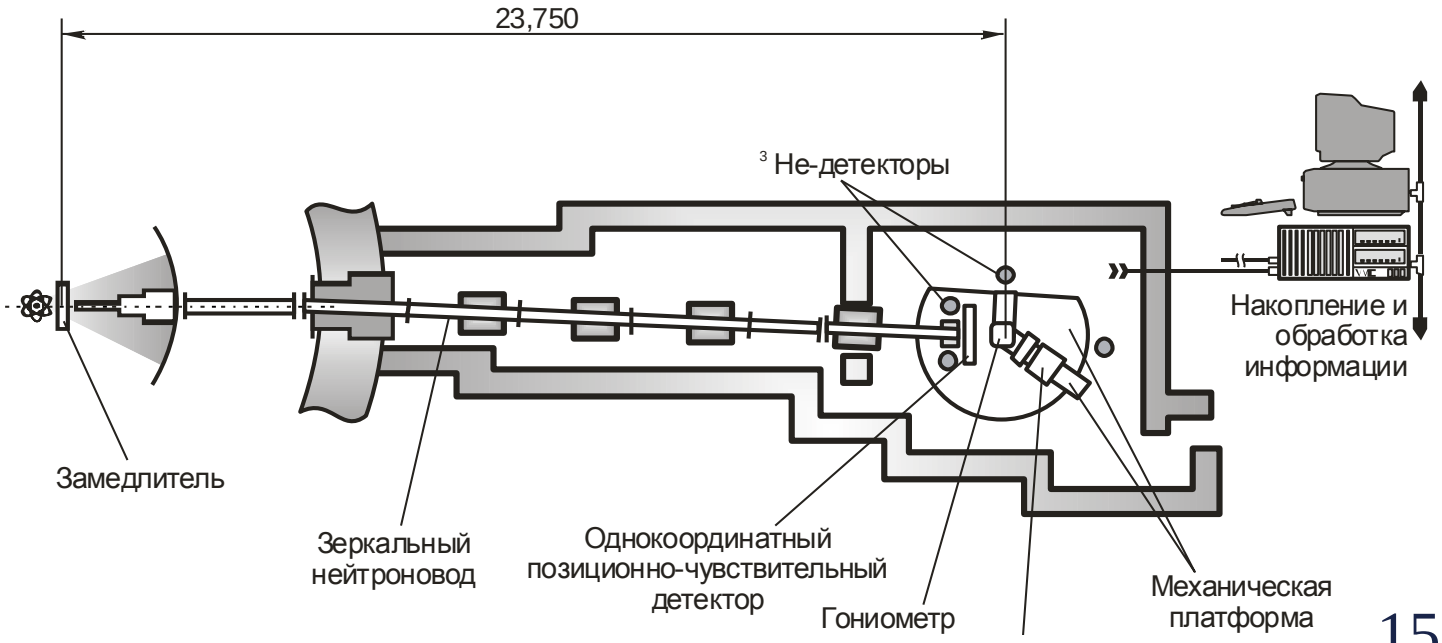

Neutron diffractometer must be optimized!

I. Single crystal experiment

2D PSD, $\Delta x \approx 0.3$ cm

II. Structural experiment with powder

high resolution, $\Delta d/d \approx 0.002$

III. Magnetic structure

medium resolution, large (~15 Å) *d*-spacings

IV. Real–time experiment

high intensity, wide *d*-spacing range

V. High-pressure experiment with microsample

high intensity, very low background

Atomic single crystal and powder structure

Analysis of single crystal structure

$\sigma(\kappa)=(2\pi)^3/V_c^2\cdot|F(H)|^2\cdot\varphi(\kappa-2\pi H)$ – scattering cross-section

$F_{hkl}=\sum_j b_j \exp\{2\pi i(hx_j+ky_j+lz_j)\}\cdot\exp(-B_j/4d^2)$ – structure factor

Fourier transformation of a periodic function $b(x, y, z)$

$b(x, y, z)\sim\sum_{hkl} F_{hkl}\cdot\exp\{-2\pi i(hx+ky+lz)\}$ – scattering density

Reverse Fourier transformation

Light elements are well visible

Scattering density can be negative

D23 single crystal diffractometer at the ILL, Grenoble. It is perfectly suited for low temperature, high magnetic field studies.

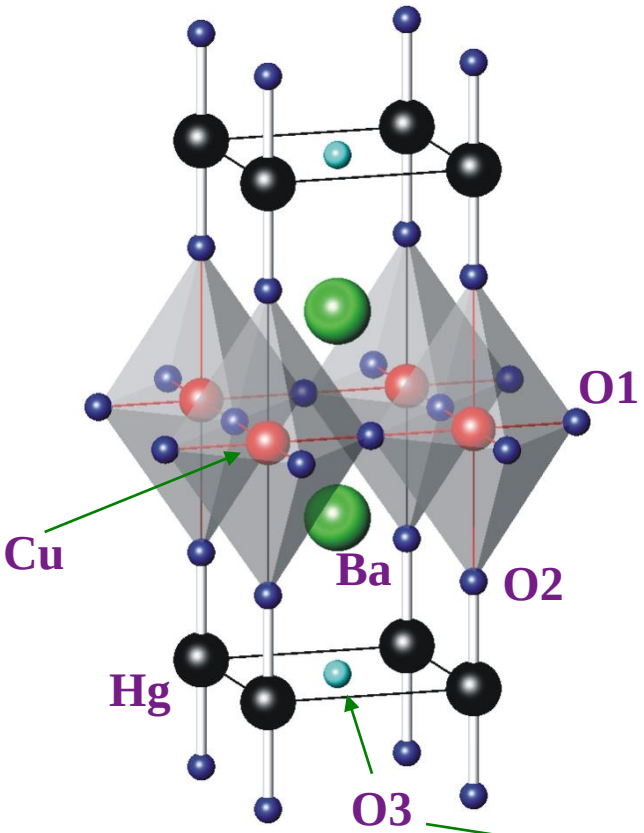

$0 \le x = y \le 1,$

$0 \le z \le 0.5$

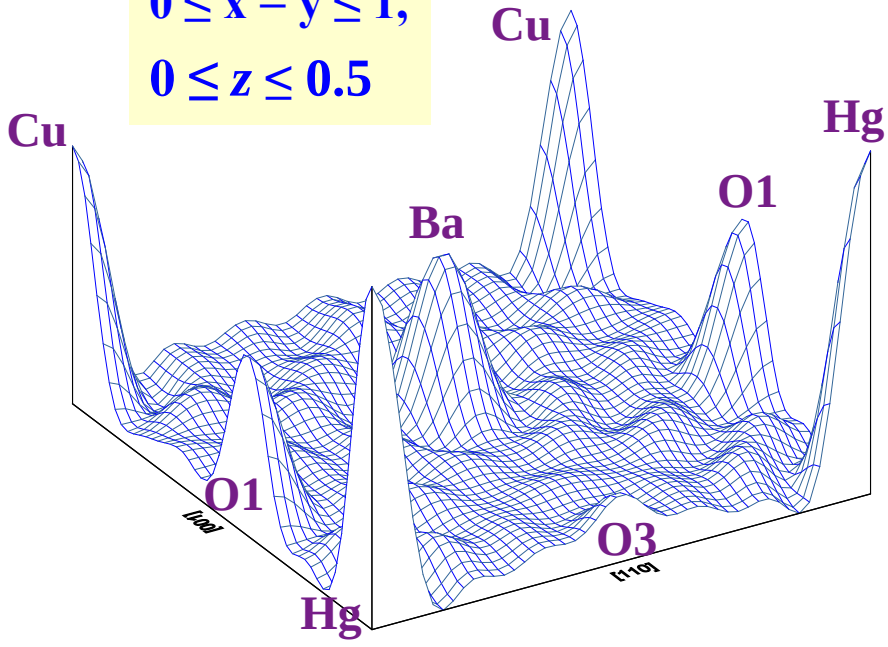

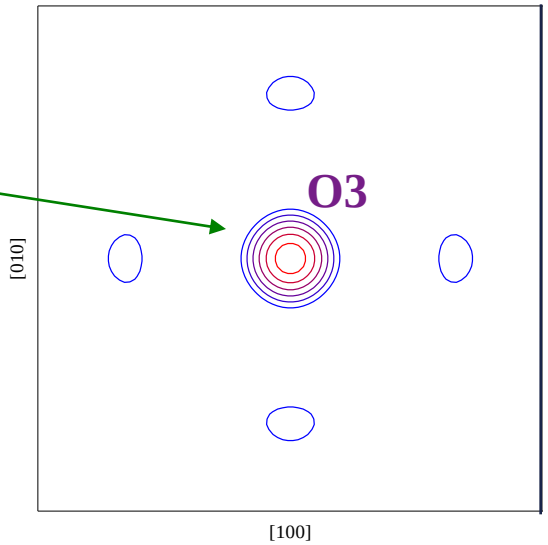

$HgBa_2CuO_{4+\delta}$ compound
O3 position is filled partly:
$n(O3) = \delta \approx 0.12.$

Difference synthesis

$0 \le x \le 1,$

$0 \le y \le 1,$

$z = 0$

Conventional parametric problem – powder structure

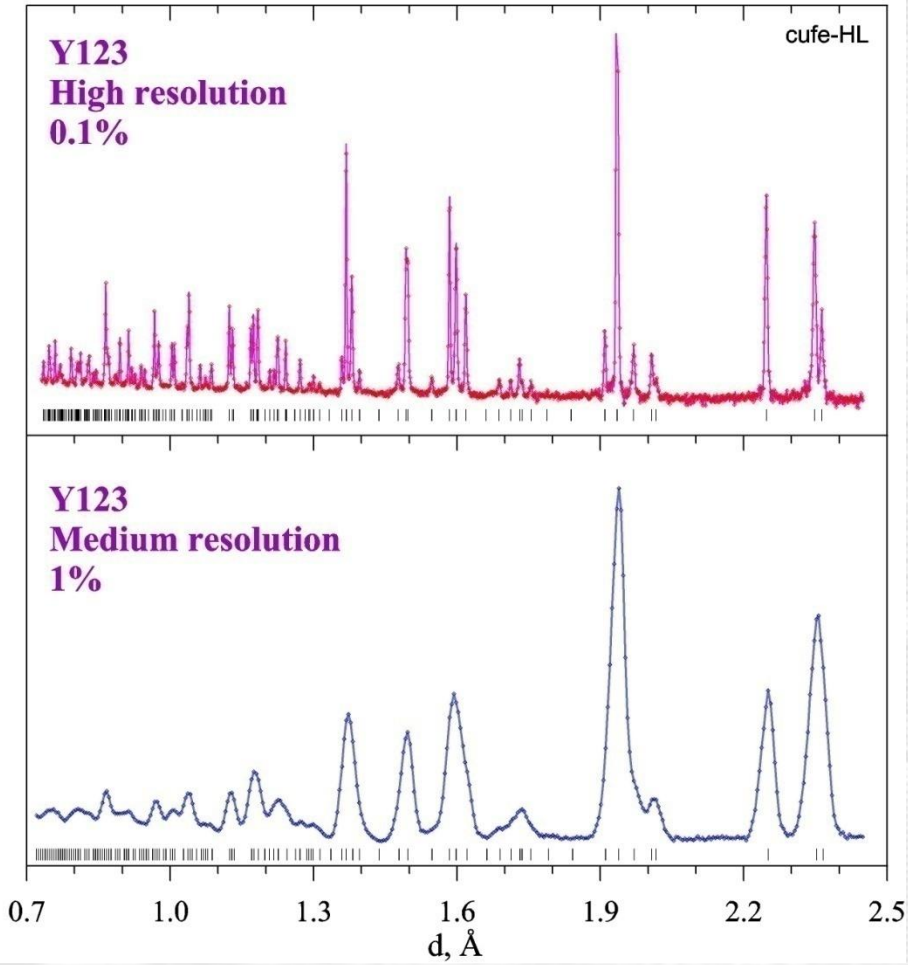

$YBa_2Cu_3O_{6+\delta}$

18 structural parameters:

(*a*, *b*, *c*) – lattice,

B_Y, $(z, B)_{Ba}$, $(n, B)_{Cu1}$, $(n, z, B)_{Cu2}$,

$(z, B)_{O1}$, $(z, B)_{O2}$, $(z, B)_{O3}$, δ.

For reliable refinement ~5 points per parameter are needed, i.e. ~90 peak intensities

High resolution in reciprocal space is obligatory!

Resolution of a neutron diffractometer

1) λ = Const	R(d) is a complicated function with a deep minimum	
2) TOF	$\Delta t_0 \sim \lambda \rightarrow$	R(d) ≈ Const
3) Fourier	$\Delta t_0 \approx$ Const $\rightarrow$	R(d) ≈ $[A^2 + (B/d)^2]^{1/2} \rightarrow A$ for large d

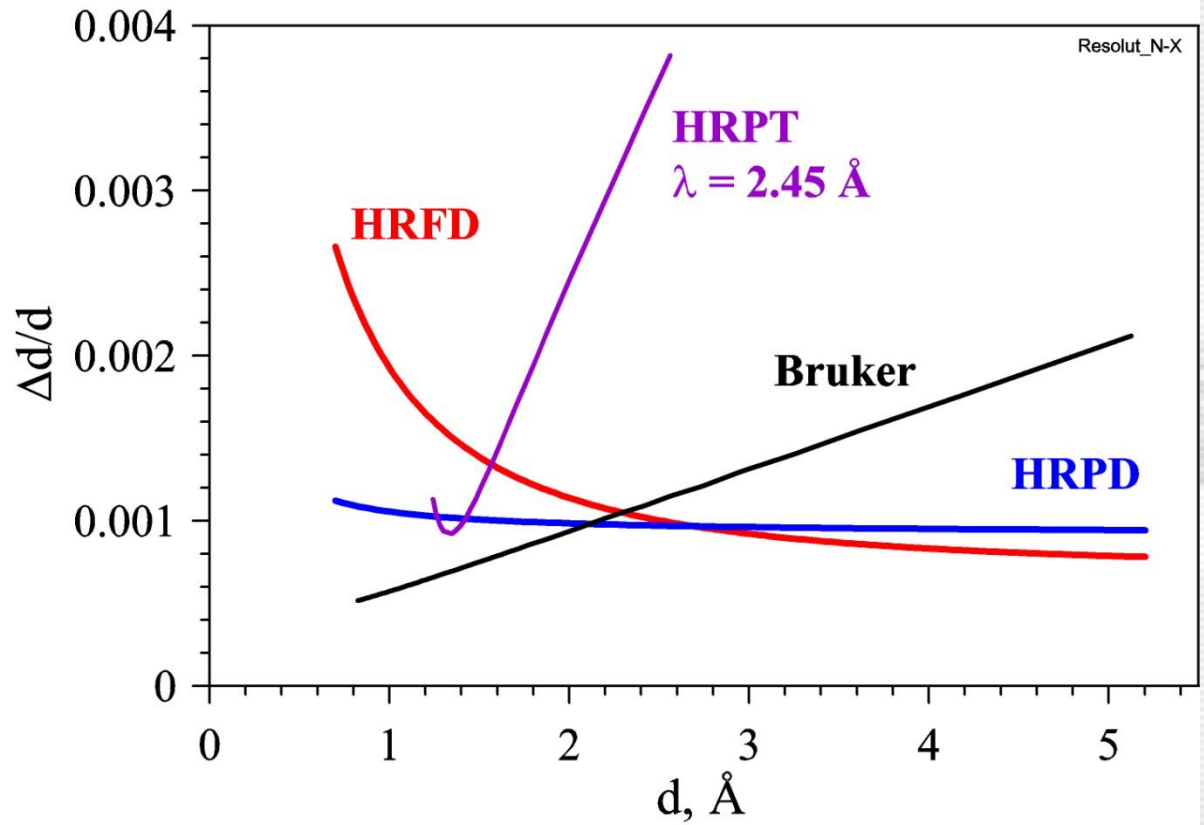

NAC-стандарт ($Na_2Al_2Ca_3F_{14}$) на TOF- и λ_0 -дифрактометрах

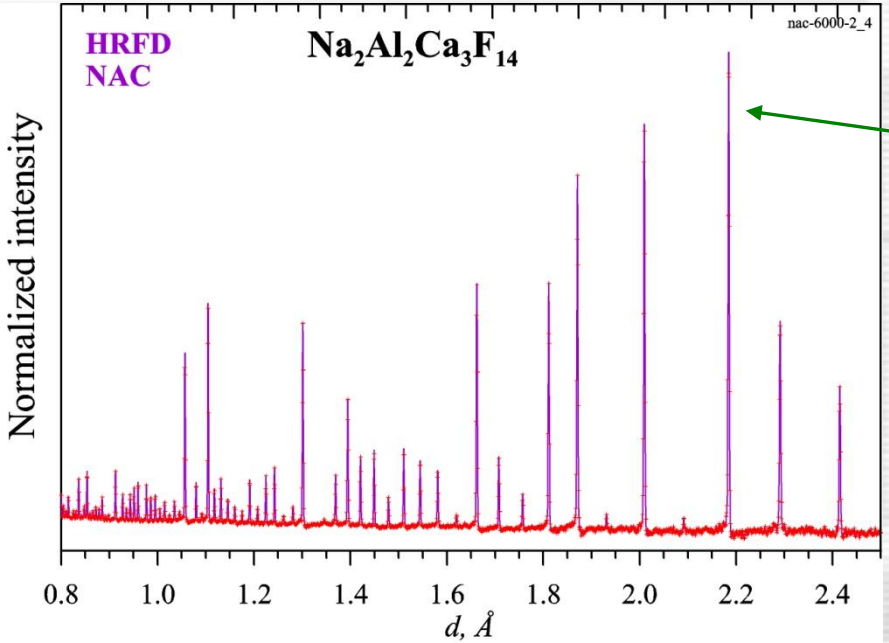

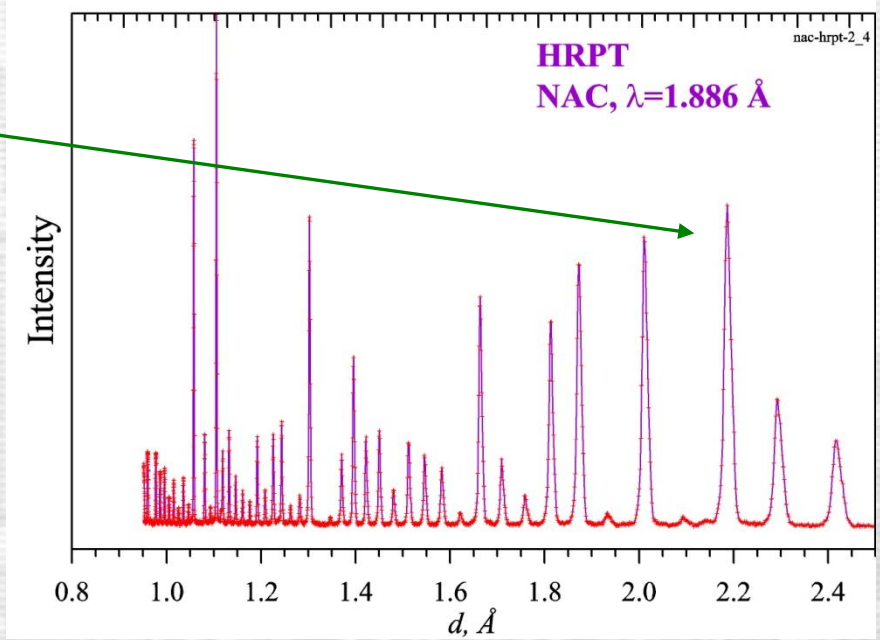

TOF diffractometer HRFD: $2\theta_0$ = 152°, wavelength range = 1.2 – 7.2 Å.

λ_0 diffractometer HRPT: λ_0 = 1.886 Å, range of scattering angles = 10 - 165°.

Refinement powder structure. The Rietveld method.

$I(d) \sim \Phi(d)A(d) \sum j_n |F_n|^2 d_n^4 \varphi(d_n - d)$ – profile function for diffraction pattern

$\chi^2 = \Sigma\, \omega_i (J_i - I_i)^2 \rightarrow \min$ – functional for minimization,

J_i are measured intensities,

I_i are calculated (according a model) intensities.

Parameters are:

$a, b, c, \alpha, \beta, \gamma$	lattice constants,
n_j	occupancies,
x_j, y_j, z_j	coordinates,
B_j	thermal factors

King Carl Gustaf of Sweden, in Stockholm, 31 March 1995 awarded Dr. Rietveld with the Aminoff prize

NAC- standard sample, R = $\Delta d/d \approx 0.001$, HRFD (IBR-2)

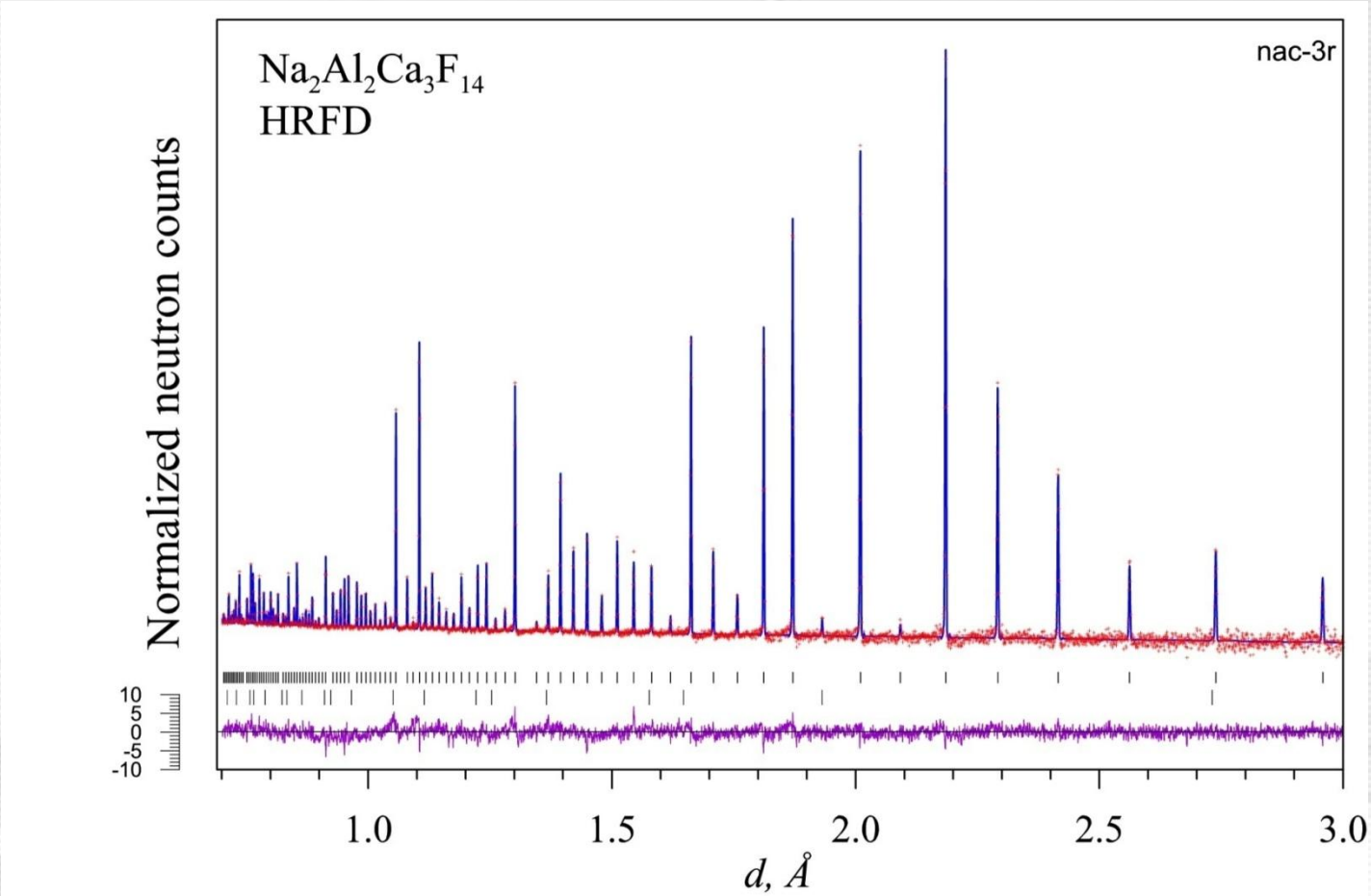

Intensities ⟶ **atomic and magnetic structure, texture**

Positions ⟶ **elementary cell dimensions, internal macrostress**

Widths ⟶ **coherent block size, internal microstress**

Microstructure: size and stress effects

$$W^2 = C_1 + C_2 d^2 + C_3 d^2 + C_4 d^4$$

Resolution function of TOF-diffractometer

Stress effect, $C_3 = (\Delta a/a)^2$

Size effect, $C_4 \sim (1/L)^2$

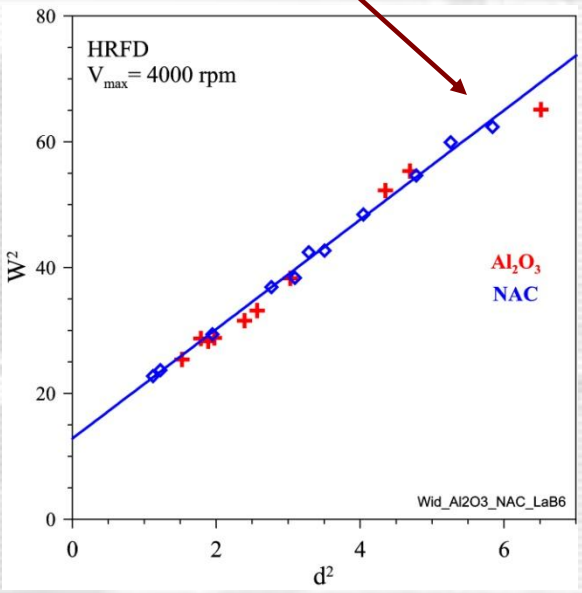

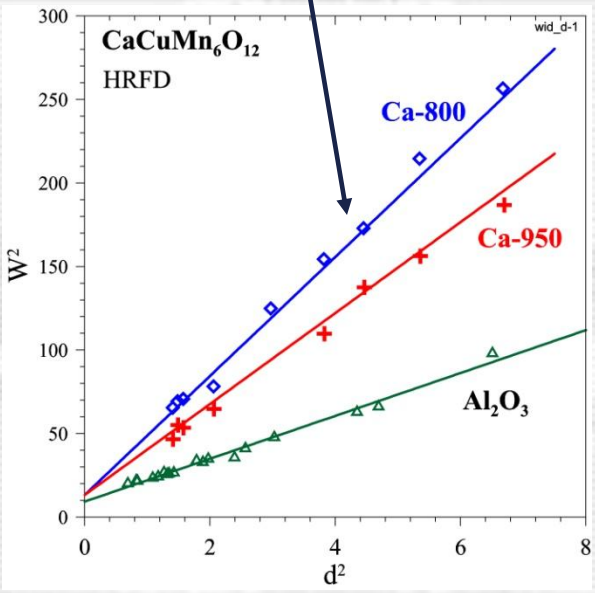

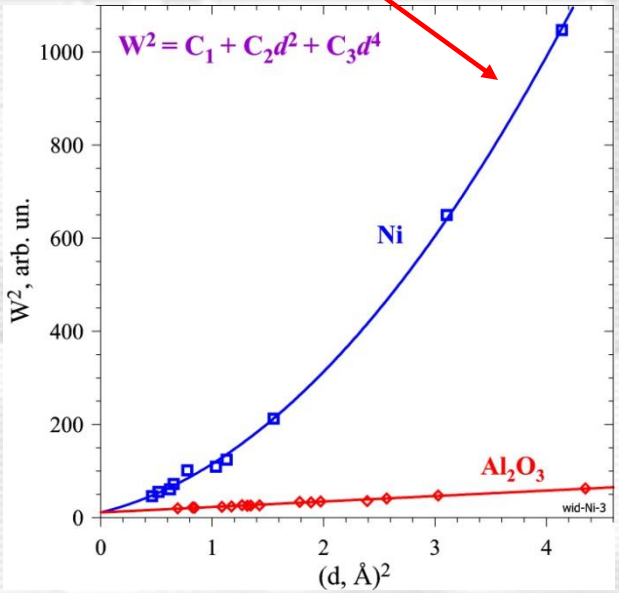

Standard samples (NAC, Al_2O_3) without stresses

Stress effect in $CaCuMn_6O_{12}$

Size effect in nanostructured Ni

HRFD: defect structure of the niobium carbide, NbC_x

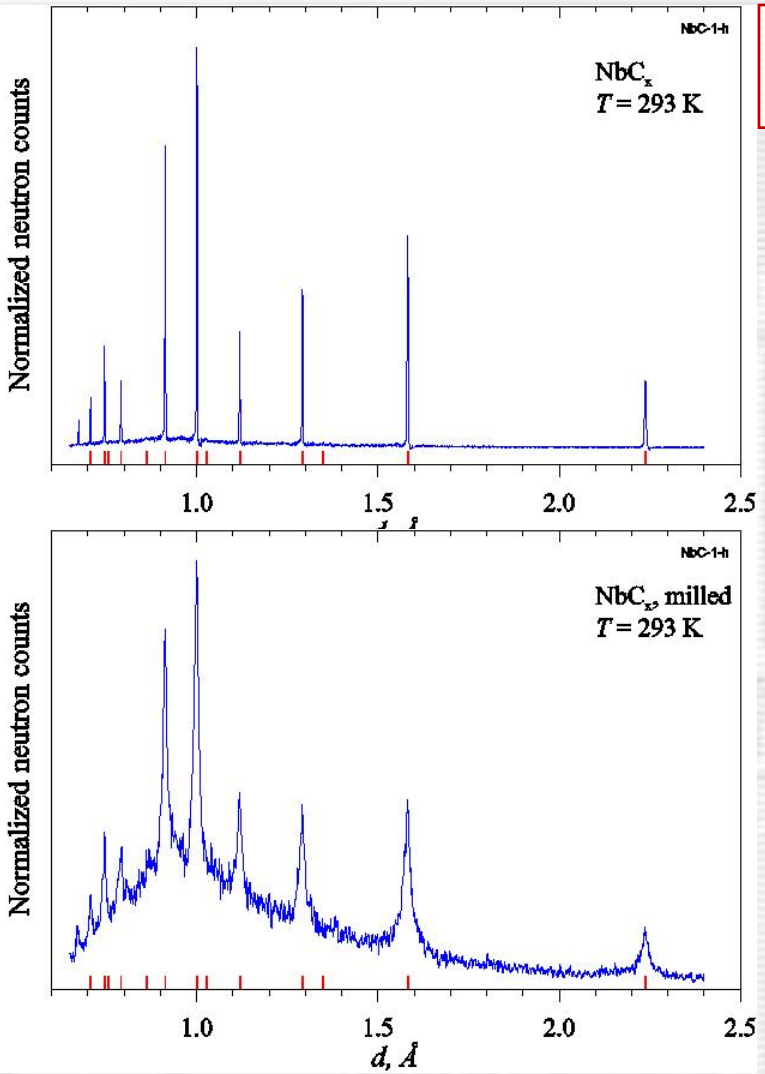

Diffraction pattern of the reference sample.
The average crystalline size is > 4000 Å, $\Delta d/d \approx 0.002$.

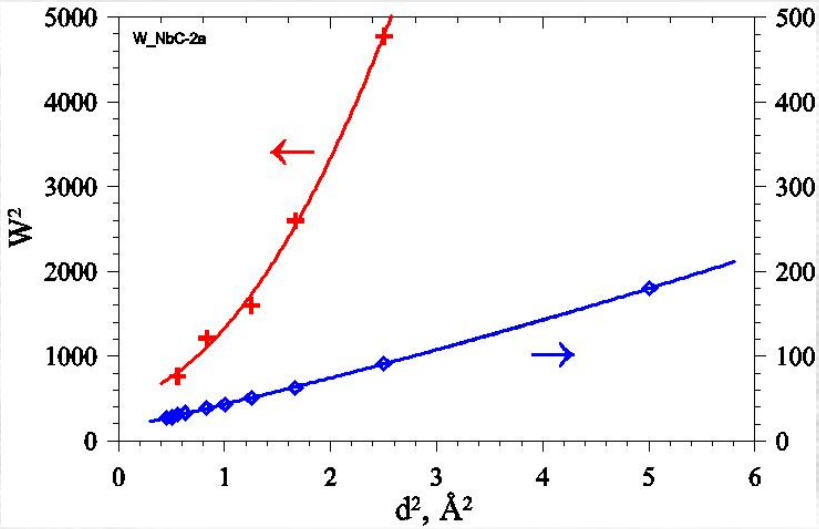

Widths of diffraction lines as a function of d-spacings for reference (blue) and milled (red) samples of NbC_x

Diffraction pattern of the fine milled sample.
The average crystalline size is ~100 Å, $\Delta d/d \approx 0.013$.

Magnetic structure

“Conventional” ordered magnetic structures

Ferromagnetic, $M \neq 0$ at $T < T_C$

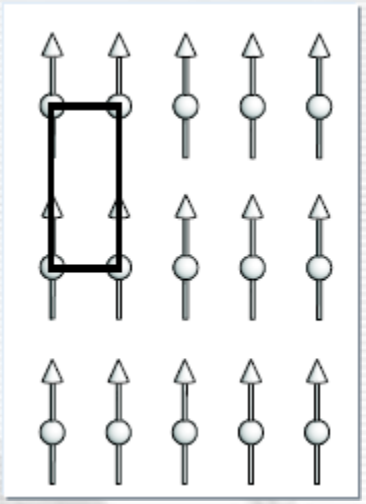

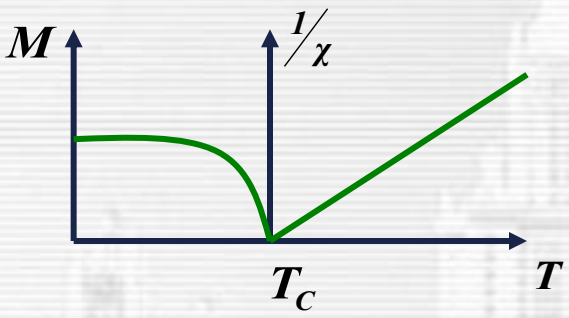

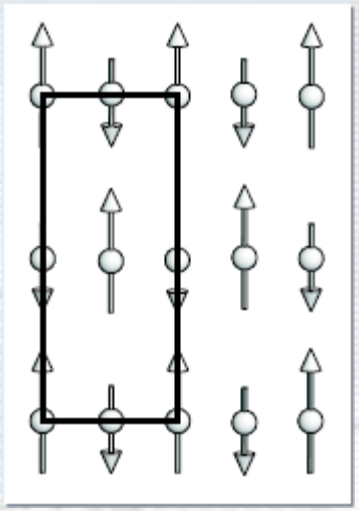

Ferrimagnetic
$\mu_1 \neq \mu_2$

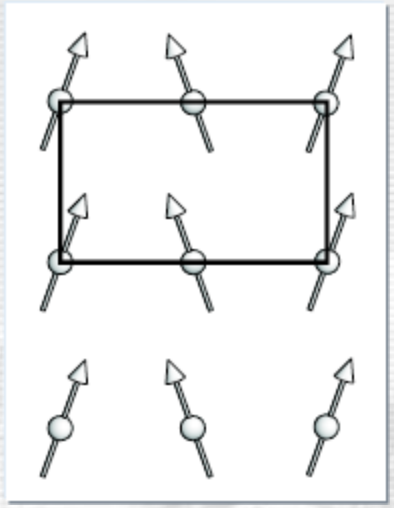

“Canted” structure

Antiferromagnetic, $M = 0$ at $T < T_N$

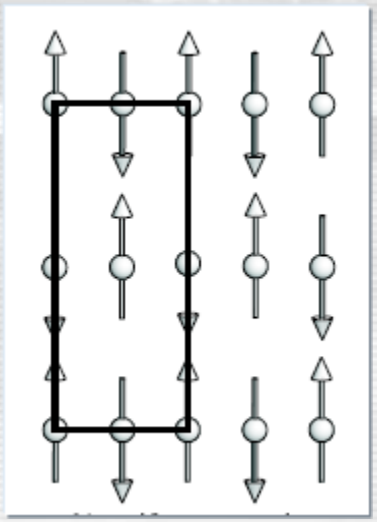

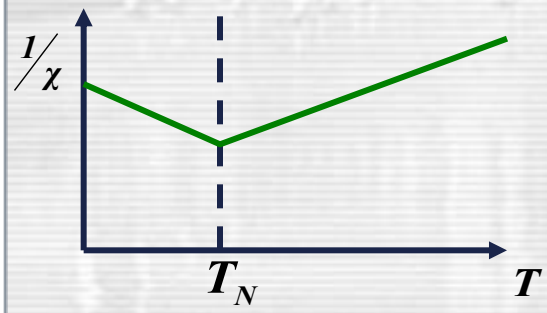

Magnetic and atomic structures are commensurate. There is a magnetic unit cell.

Pictures are from “Magnetic Structure – Group Theory” of *Andrew S. Wills*

“New” ordered and incommensurate magnetic structures

Geometrically frustrated magnets

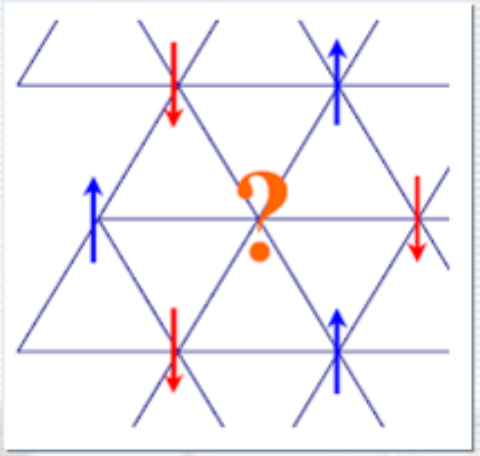

Triangular lattice: $YMnO_3$

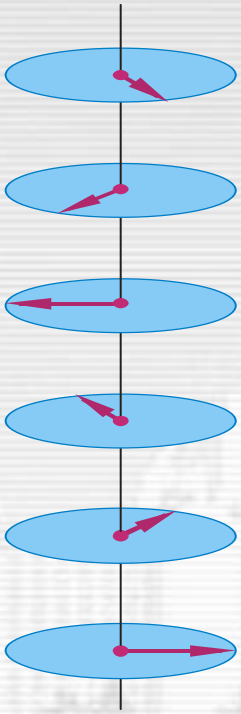

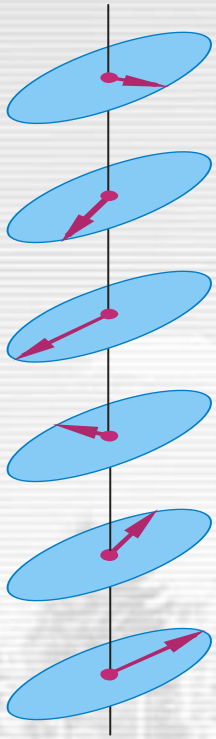

Circular helix
Au_2Mn,

Inclined helix

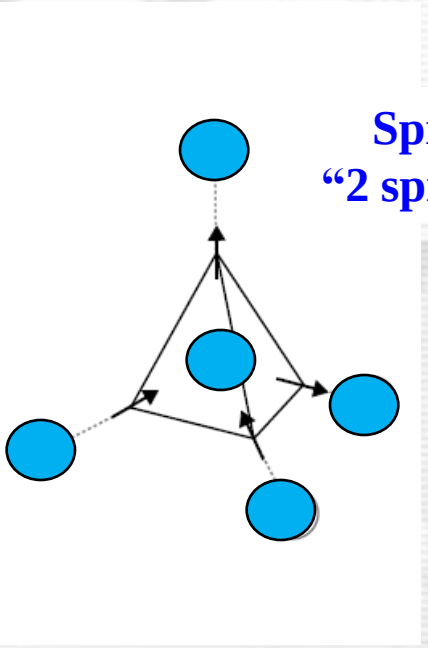

Spin ice: $Ho_2Ti_2O_7$
“2 spins in, 2 spins out”

Magnetic and atomic structures are incommensurate, T_m/T_a is not rational, $T_m >> T_a$

Typical magnetic neutron powder diffraction pattern

$(La_{0.2}Pr_{0.8})_{0.7}Ca_{0.3}MnO_3$, DMC instrument, SINQ (PSI)

T_N = 130 K, T_C = 100 K, at T < 80 K: FM (85%) + AFM_{CE}(15%)

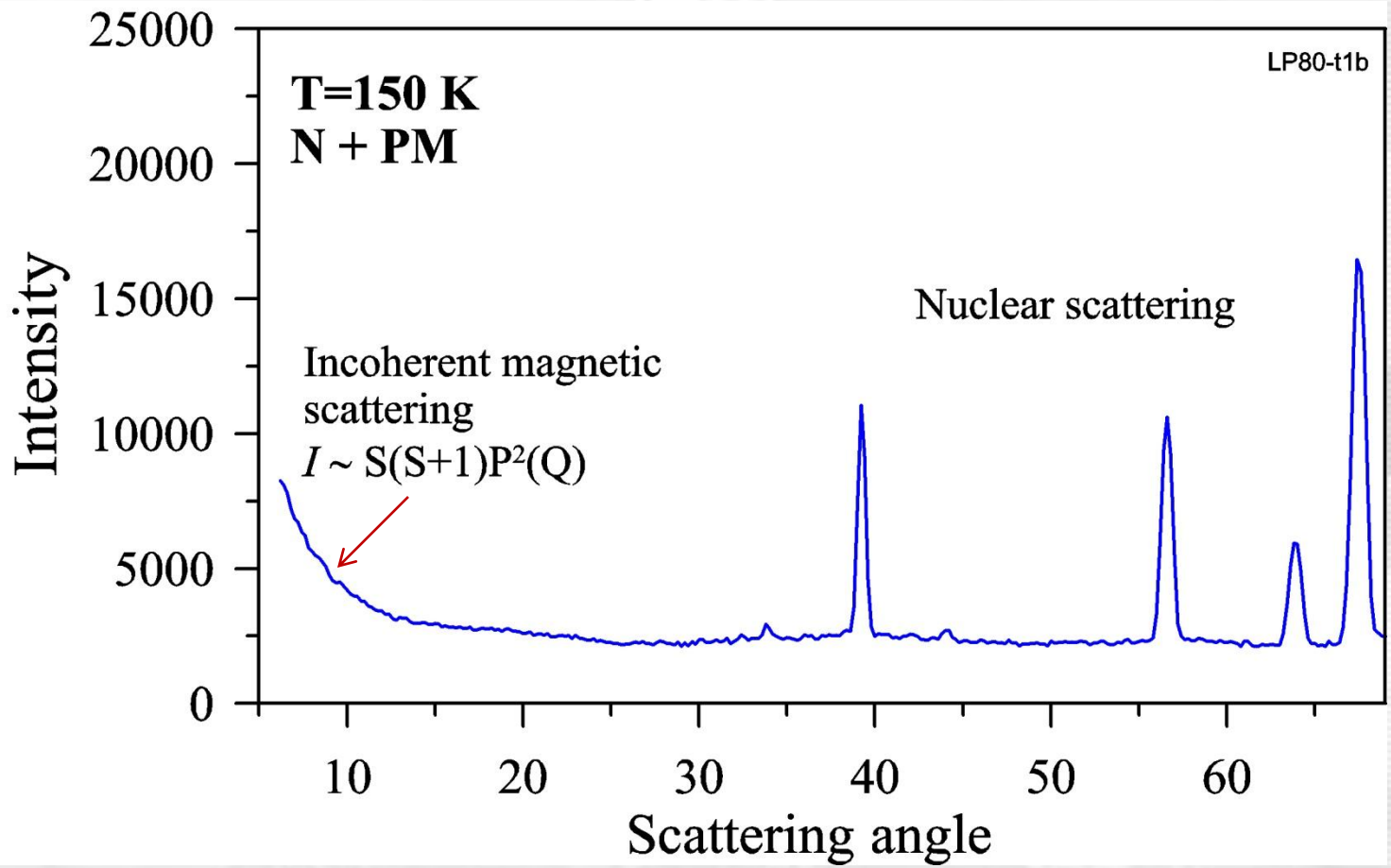

$T > T_N$, nuclear + paramagnetic scattering

Typical magnetic neutron powder diffraction pattern

$(La_{0.2}Pr_{0.8})_{0.7}Ca_{0.3}MnO3$, DMC instrument, SINQ (PSI)

T_N = 130 K, T_C = 100 K, at T < 80 K: FM (85%) + AFM_{CE}(15%)

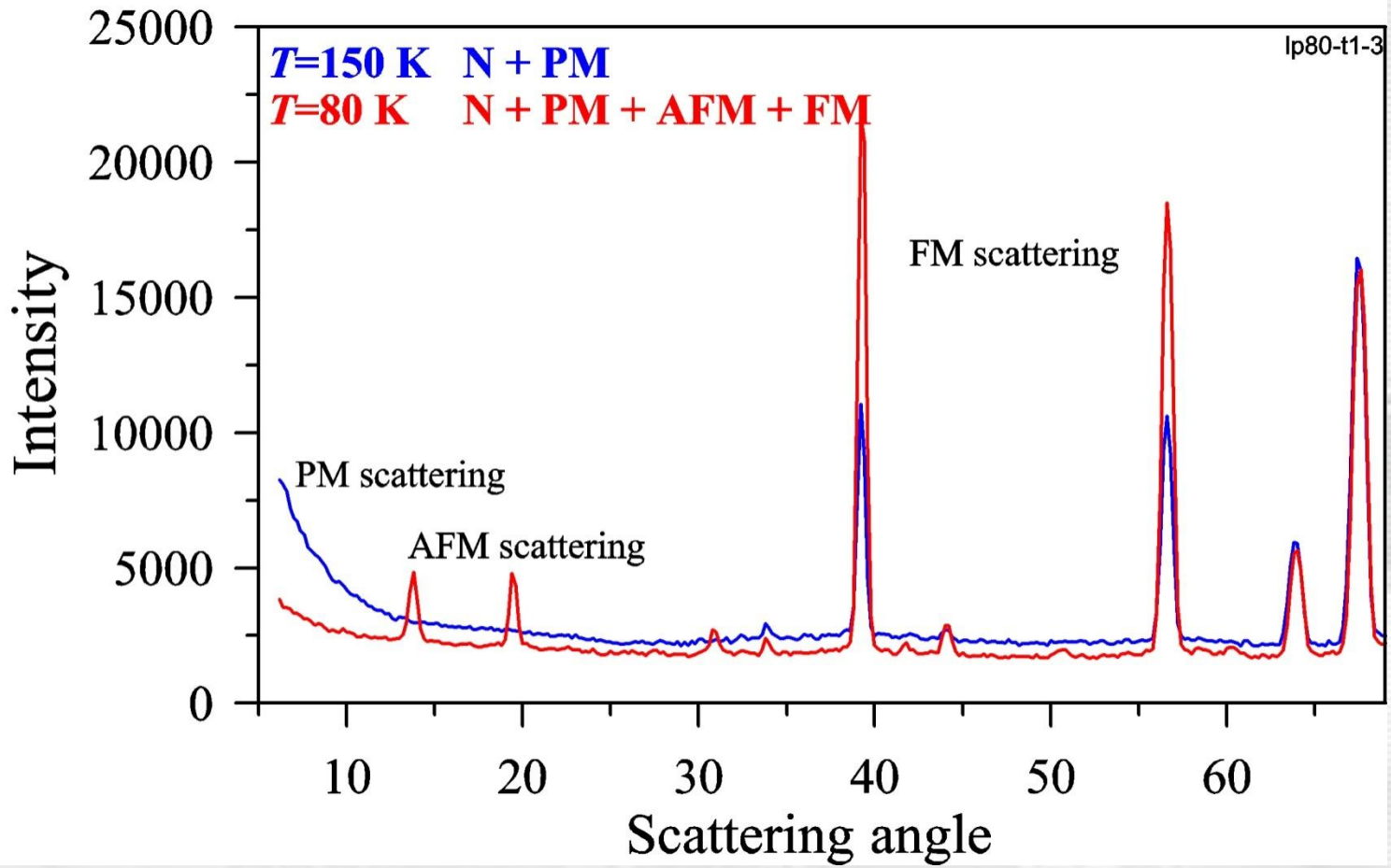

$T < T_C$, two phases (FM + AFM) state

Real time studies

Transitional phenomena & TOF diffraction / SANS

Irreversible process

characteristic time (τ)
~ (1 s – 1 hour)

1. Solid state chemical reaction
2. Isotope exchange
3. Phase transitions

Reversible process

1. Slow τ ~ 10 – 1000 ms
2. Fast τ ~ 100 – 1000 μs
3. Very fast τ ~ 10 μs

1. Polarization reversal
2. First order phase transition
3. New equilibrium state induced by an external field

High-intensity and high-resolution diffraction with λ = const diffractometer

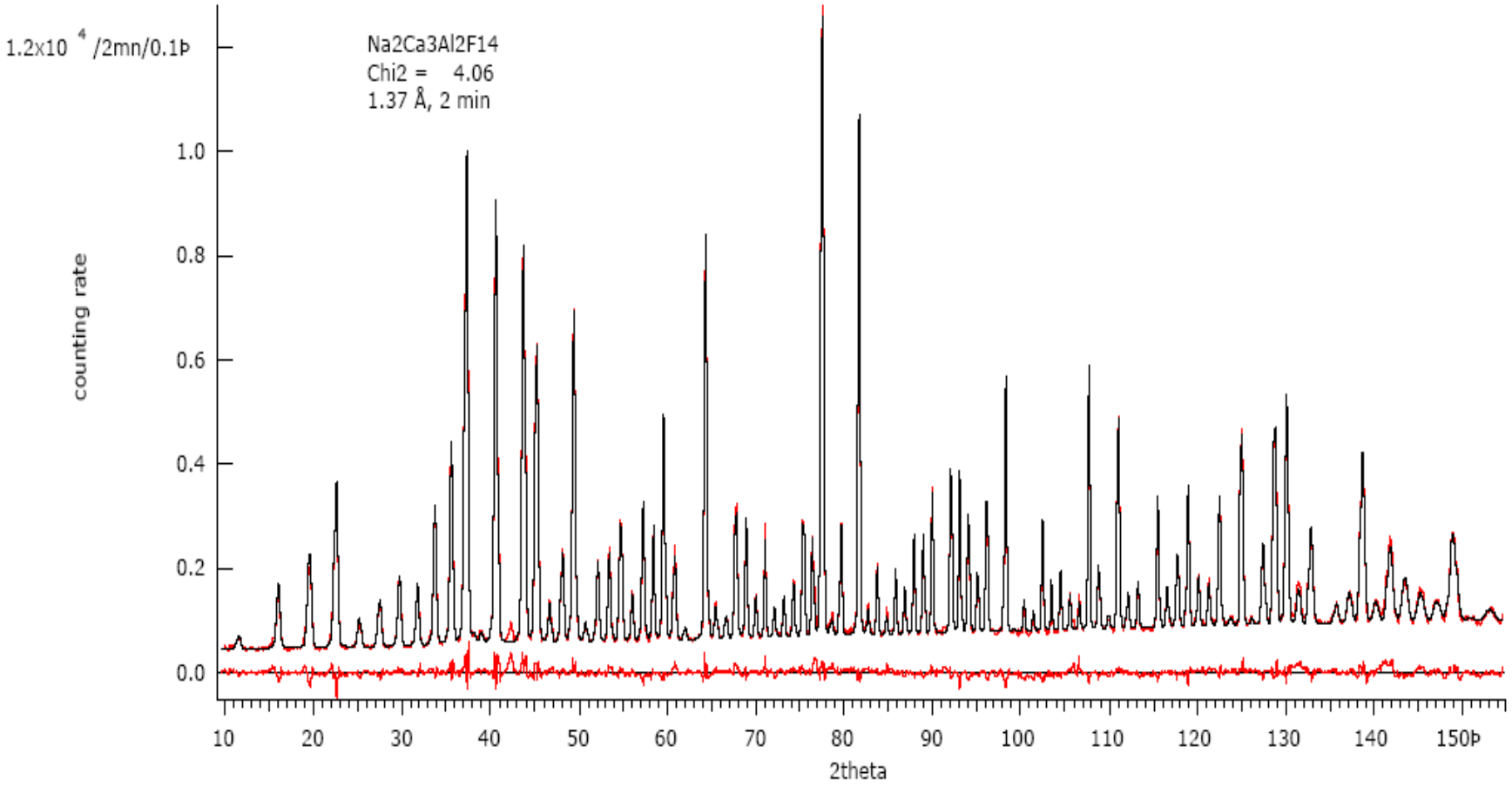

Diffraction pattern obtained in 2 minutes on D20 (ILL) in high-resolution mode. NAC-standard, Hansen et al. 2003.

Self-propagating high-T synthesis of titanium silicon carbide Ti_3SiC_2

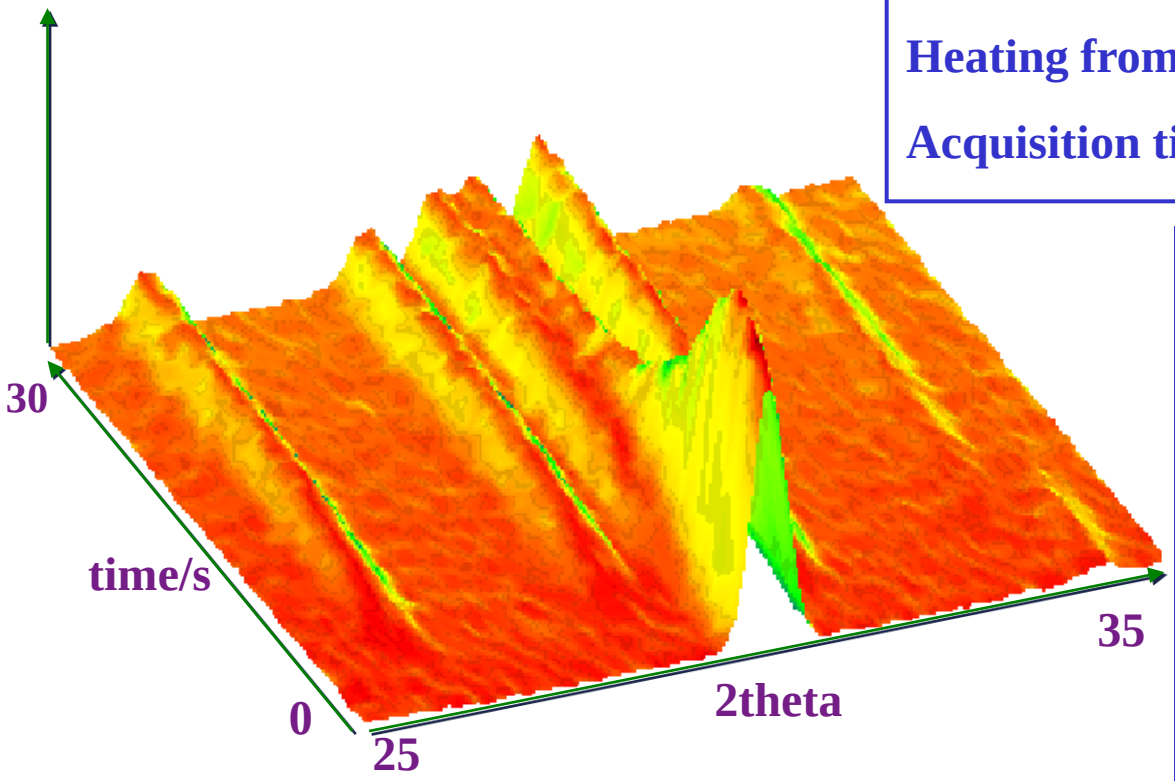

3 Ti : 1 Si : 2 C, 20 g pellet in furnace

Heating from 850 C to 1050 C at 100 K/min

Acquisition time 500 ms (300 ms)

Ti α-β transition
- starting at 870 C

Pre-ignition:
- TiC_x growth during 1 min

Melting (?) in 0.5 s

Intermediate phase
- TiC, Si substituted
- formed in 0.5 s, 2s delay
- heating up to 2500 K
- afterwards decay in 5 s

Product Ti_3SiC_2
- starts after 5 s incubation
- time constant about 5 s

D.P. Riley, E.H. Kisi, T.C. Hansen and A. Hewat, *J. Am. Ceramic Soc.* 85 (2002) 2417-2424.

Phase transformations of high pressure heavy ice VIII. Time-resolved experiment with Δt = 5 min.

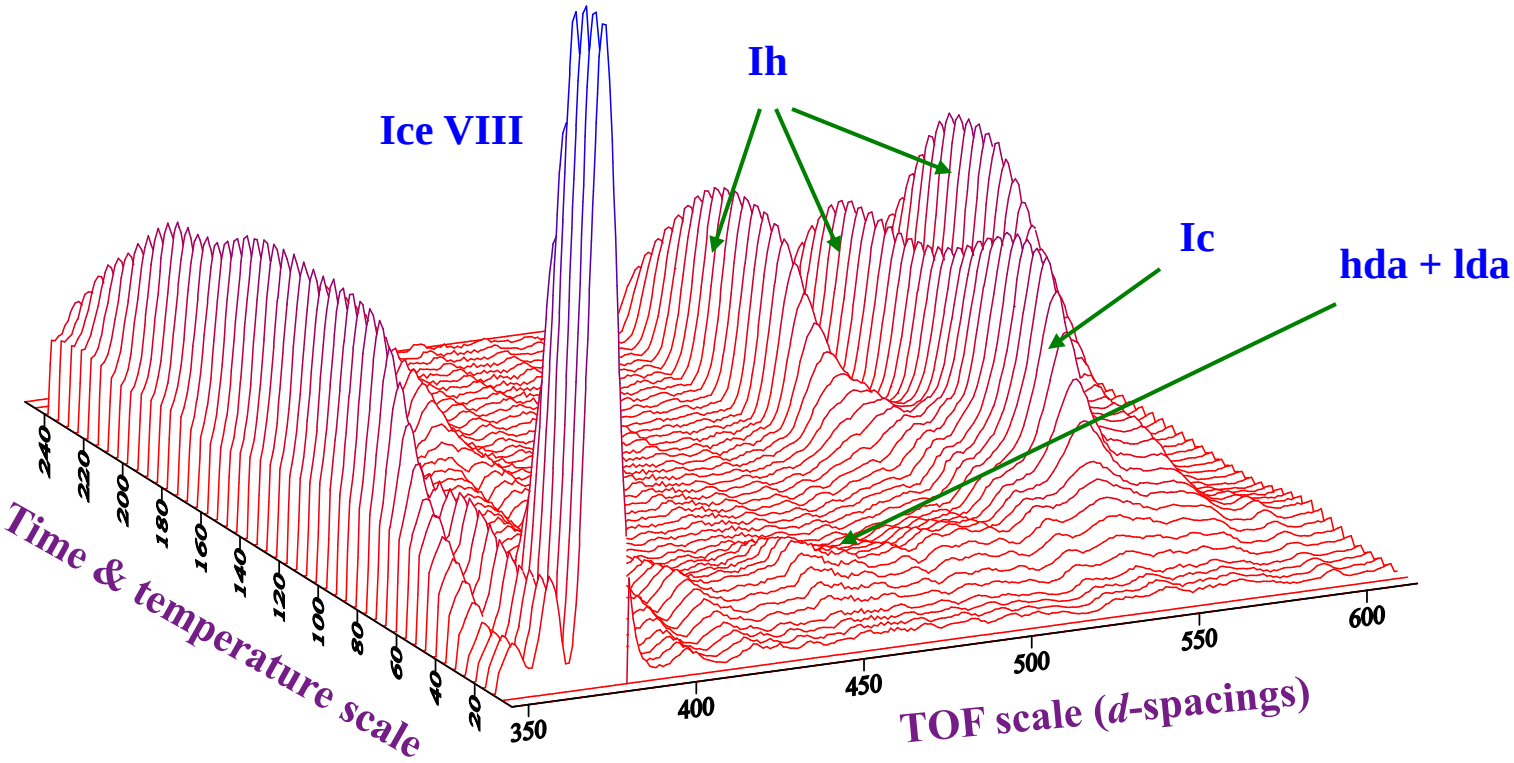

Time / temperature scale: T_{start}=94 K, T_{end}=275 K. The heating rate is ≈1 deg/min.
Diffraction patterns have been measured each 5 min. Phase VIII is transformed into high and low density amorphous phases hda + lda, then into cubic phase Ic, and then into hexagonal ice Ih.

Phase transformations in $BiSrCaCu_2O_x$ (melt-quenching, heating, melting, cooling down). First combined diffraction – SANS study (1988) with Δt=5 min.

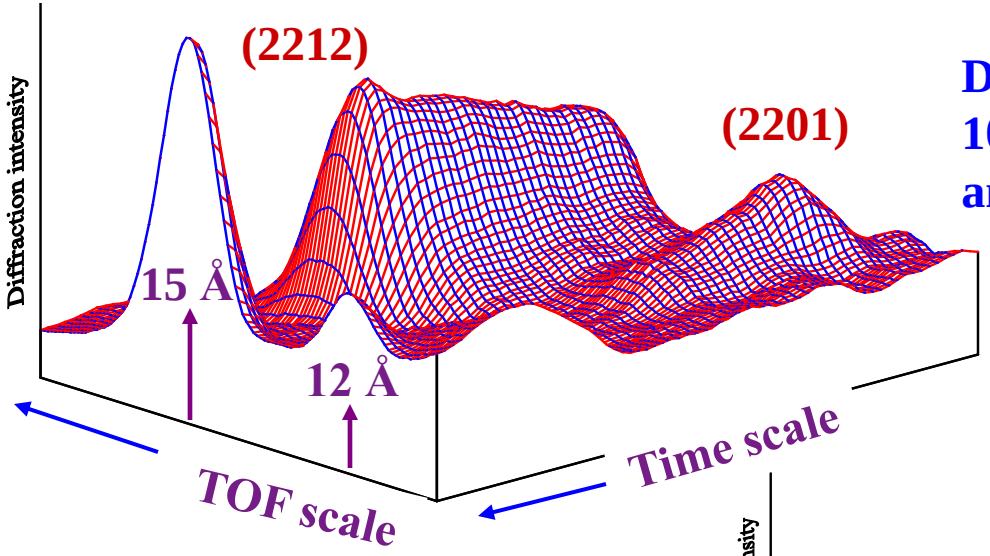

Diffraction intensity. d_{hkl} range is 10 – 18 Å. (002) peaks for (2201) and (2212) phases are seen.

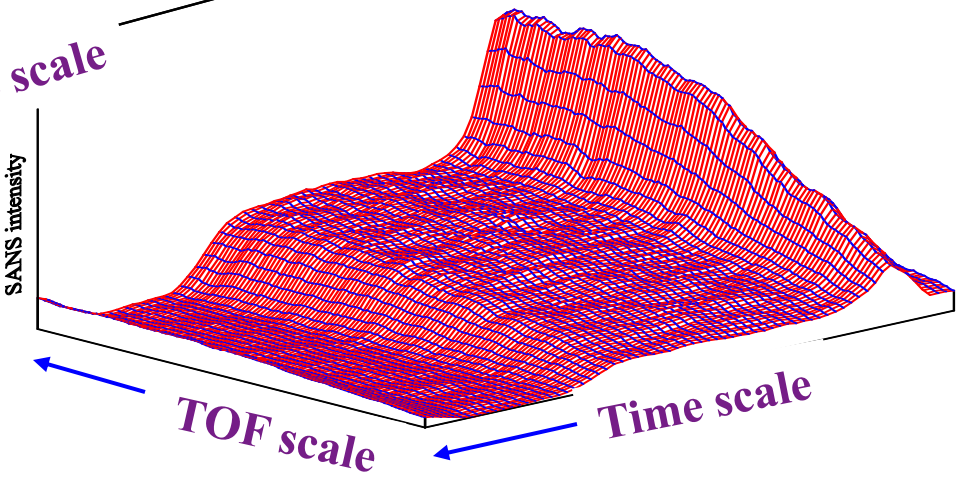

SANS intensity
Q range is 0.02 – 0.06 Å^{-1}

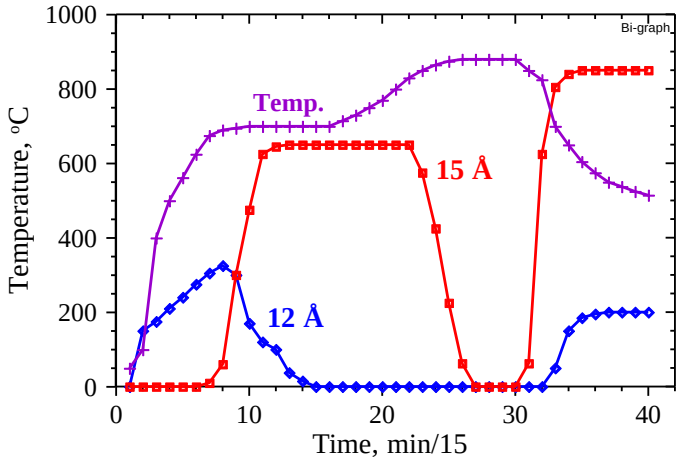

Temperature & Intensities changes

A.M.Balagurov, G.M.Mironova, MS Forum, 1993.

Nano-objects: artificial and natural

β-Ni(OH)$_2$ nanostructure

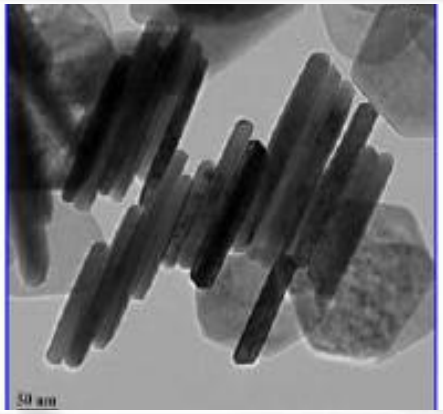

Multilayer lipid structure

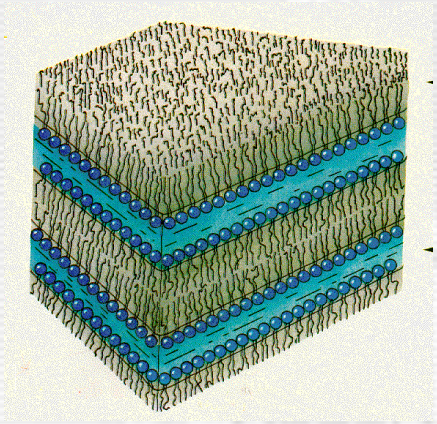

Nanoporous matrix

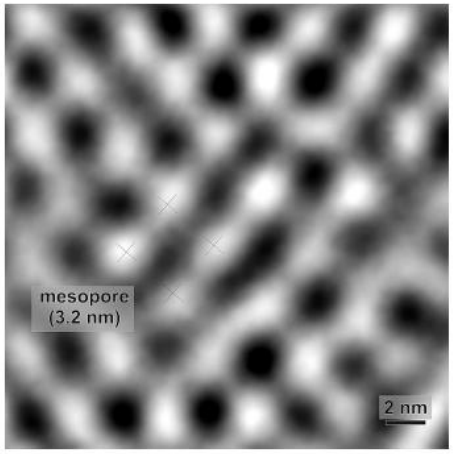

Phase separation in magnetic oxides

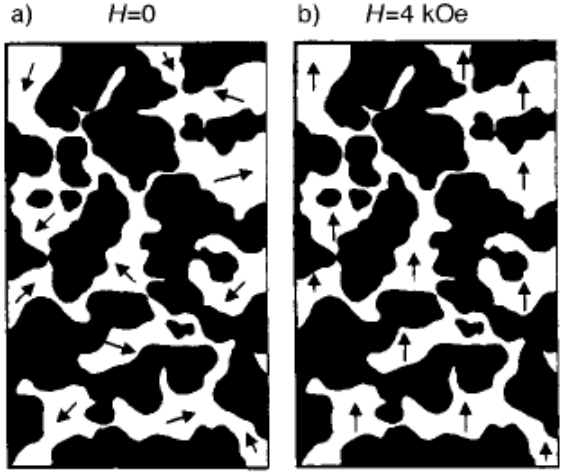

Nano-objects are characterized by:

- **dimensions (~10 nm),**
- **enhanced imperfection,**
- **self-assembling tendency**

All these properties can be investigated by using neutron scattering!

One-dimensional long-period structures

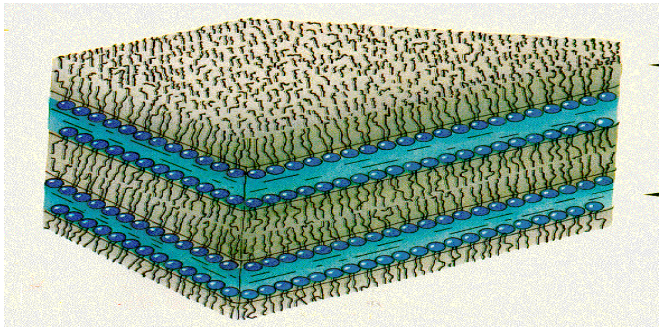

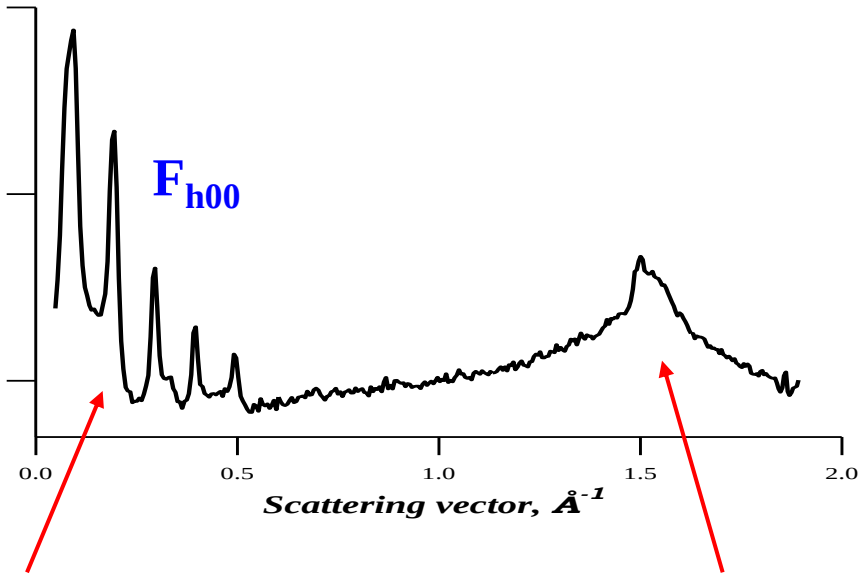

Ламеллярная дифракция

Латеральная дифракция

Gel phase $L_{\beta'}$

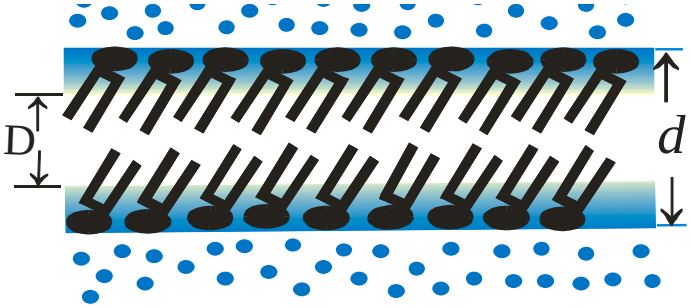

Rippl phase $P_{\beta'}$

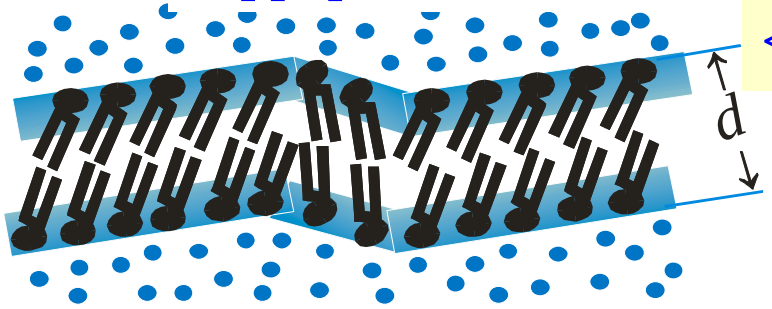

$$F_{h00} \sim \iiint b(x,y,z)\, e^{2\pi i h x} dx dy dz = \int e^{2\pi i h x} dx \iint b(x,y,z) dy dz$$

$$= \int \langle b(x) \rangle\, e^{2\pi i h x} dx$$

$$\langle b(x) \rangle = \iint b(x,y,z) dy dz = c_1 + c_2 F_{h00} \cos(2\pi i h x / d_0)$$

$$F_{h00} \sim (I_{h00})^{1/2}$$

Stratum Corneum and DMPC lipid multilayer structure

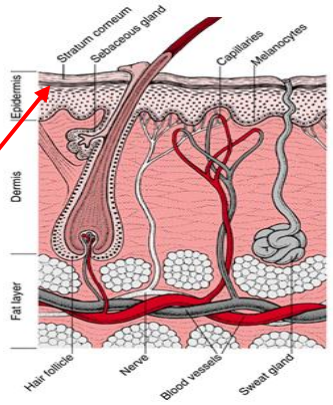

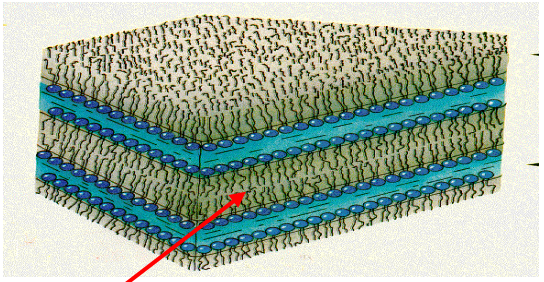

Stratum Corneum ceramide membrane.
Repeat distance 45.63 0.04Å

DMPC model membrane.
Repeat distance 54.75 0.03Å

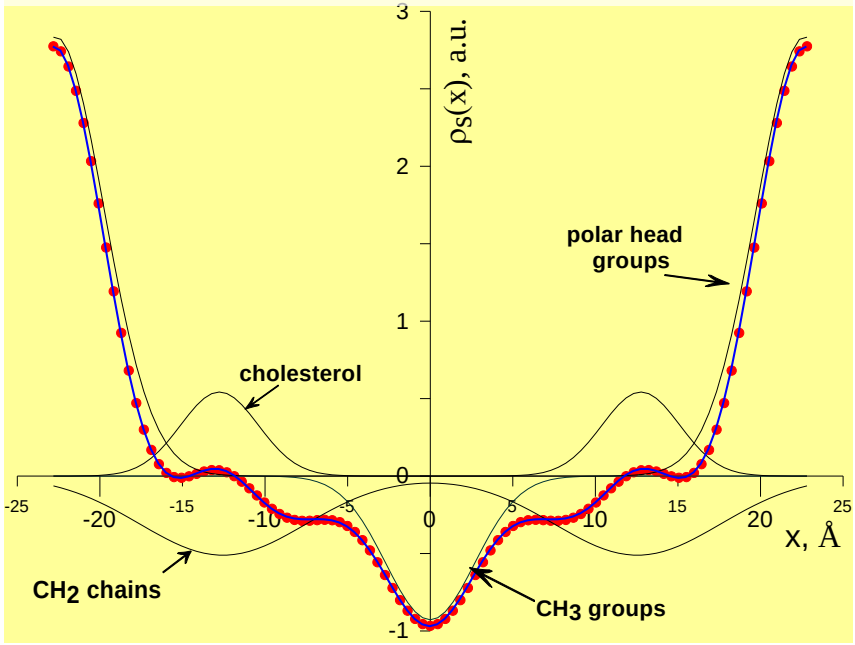

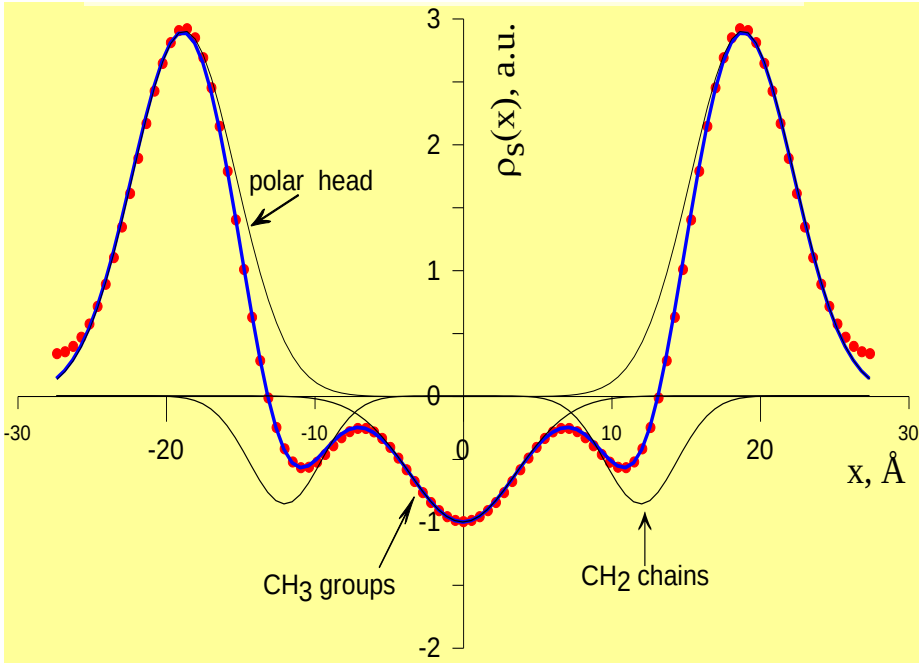

Magnetic ordering in nanoporous matrix

Nanoporous silica MCM-48 matrix

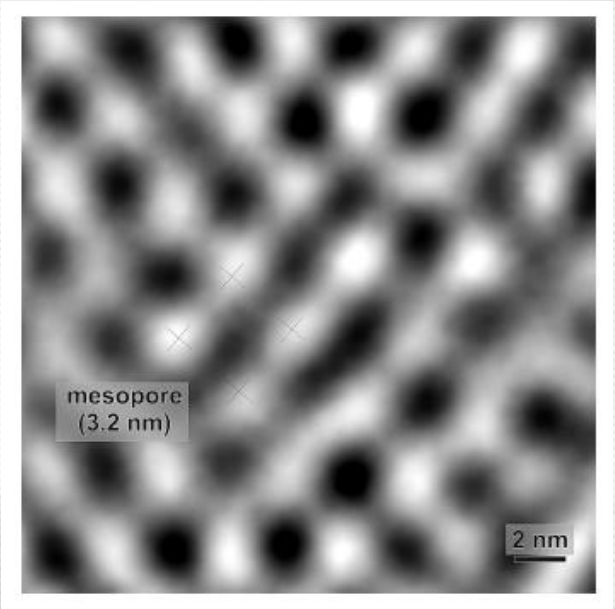

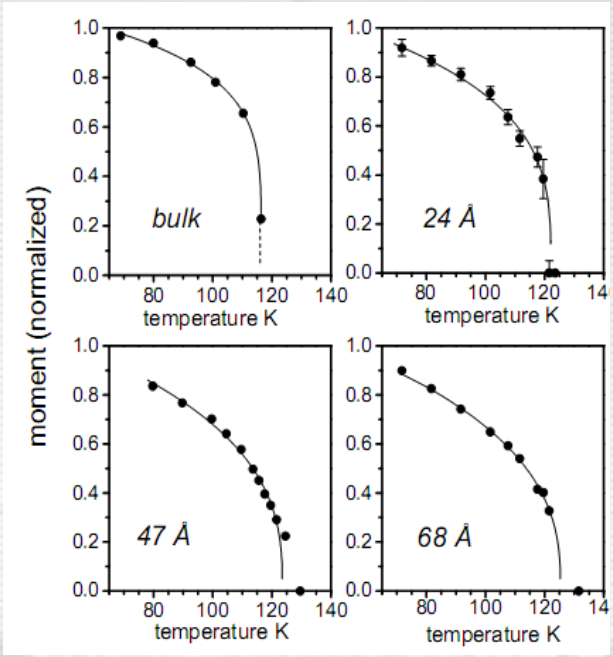

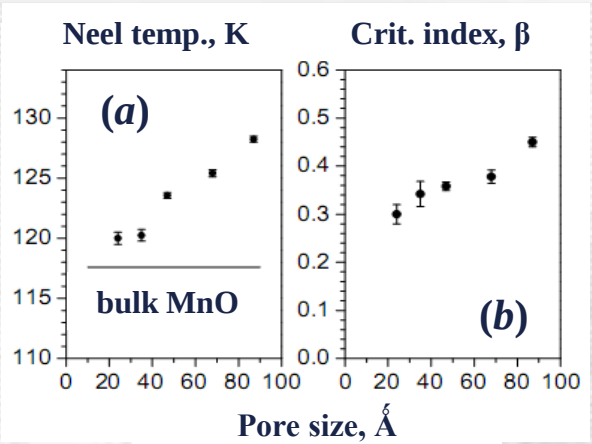

Dependencies of MnO normalized magnetic moment (left), Neel temperature and critical exponent index (right) on pore size.

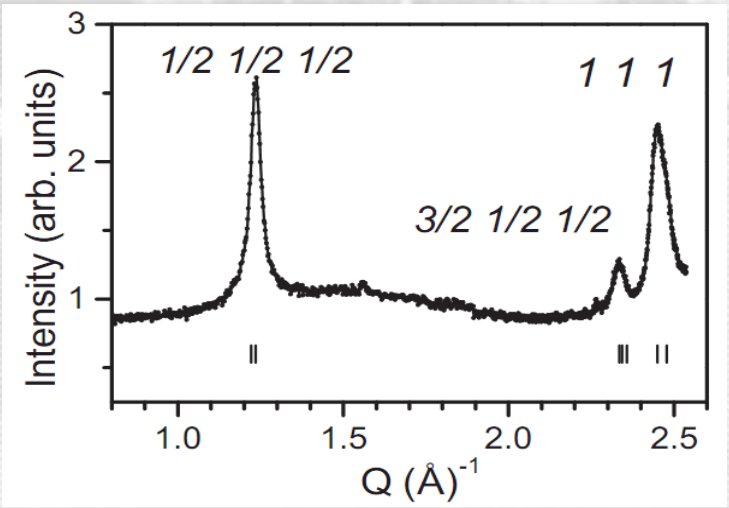

Neutron diffraction pattern of MnO inside a 47 Å pore matrix. AFM lines are clearly seen.

I. V. Golosovsky et al., PRB 72, 144409 (2005)

Neutron scattering and electrochemistry

Problems, which can be solved with neutron scattering:

- **atomic and magnetic structures of new materials (*ex situ*)**
- **phase transitions in electrode materials**
- **structural changes in electrodes in the course of redox-processes (*in situ*)**
- **structural processes in electrodes in real units (*in situ*)**
- **…**

Light atoms and cations distribution

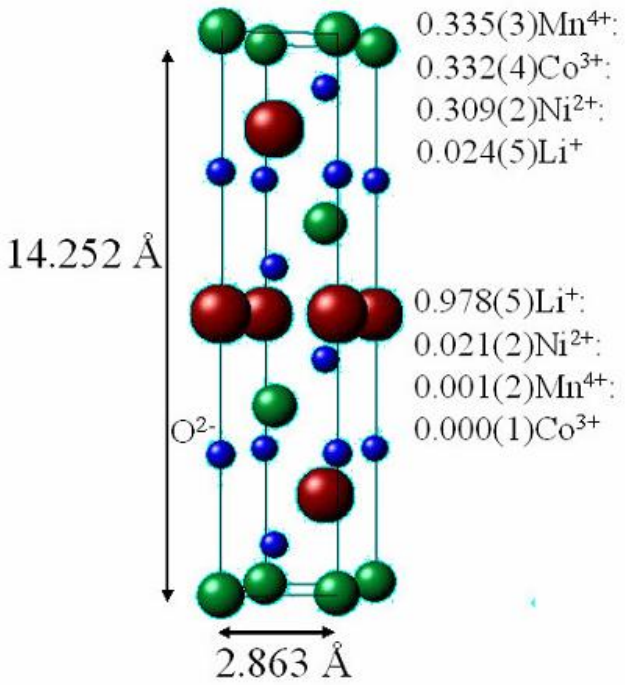

$LiMn_{1/3}Ni_{1/3}Co_{1/3}O_2$ (R-3m)

Joint synchrotron and neutron refinement. About 2% Ni displaced Li from the (3a) site.

97% Li, 3% Ni

11% Mn, 24% Ni, 10% Co, 55% Li

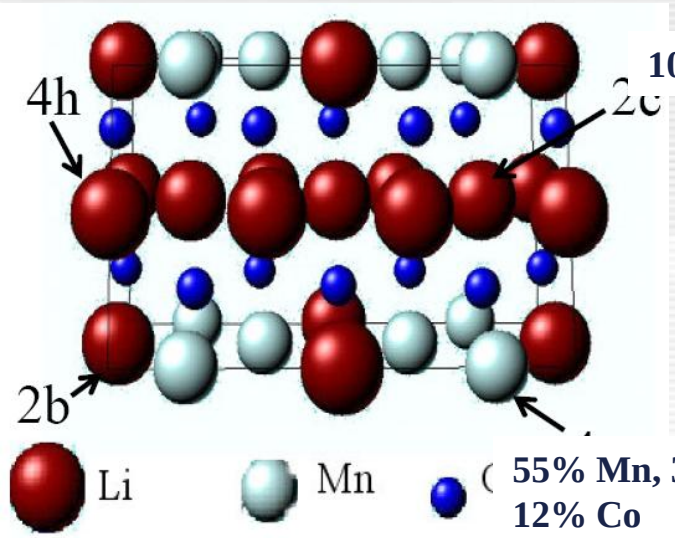

100% Li

55% Mn, 33% Ni, 12% Co

Crystal structure of Li_2MnO_3 type.

Real composition is $Li_{1.2}Mn_{0.4}Ni_{0.3}Co_{0.1}O_2$

from P.S. Whitfield et al.

Neutron diffraction cells for studying insertion processes in electrode materials

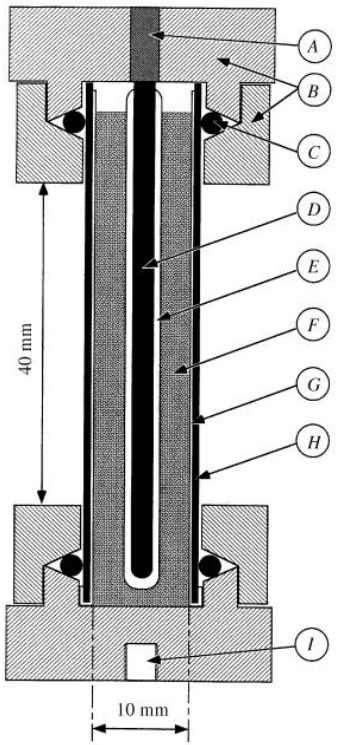

Seal for the lithium anode

Brass collars

NBR O ring

Lithium anode (diameter 2 mm)

Solid polymer electrolyte

Mixture of $LiMn_2O_4$

Gold layer, thickness ~100 nm

Pyrex tube, wall thickness 0.5 mm

Connector to neutron diffractometer

from O. Bergstom et al., J. Appl. Cryst., 1998

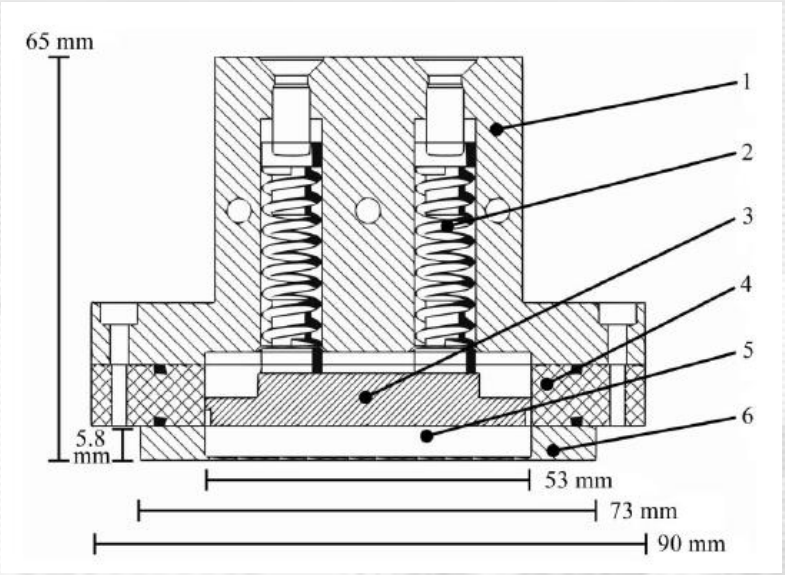

Cross section of the assembled device: (1) cell top, (2) spring with piston, (3) negative current collector, (4) cell body, (5) compartment for the active material and entry window for neutrons, (6) positive current collector.

from Fabio Rosciano et al., J. Appl. Cryst., 2008

In Situ Neutron diffraction study of the electrodes in a commercial (Saehan Enertech, Inc) Li-ion cell, HIPPO, LANSCE, USA

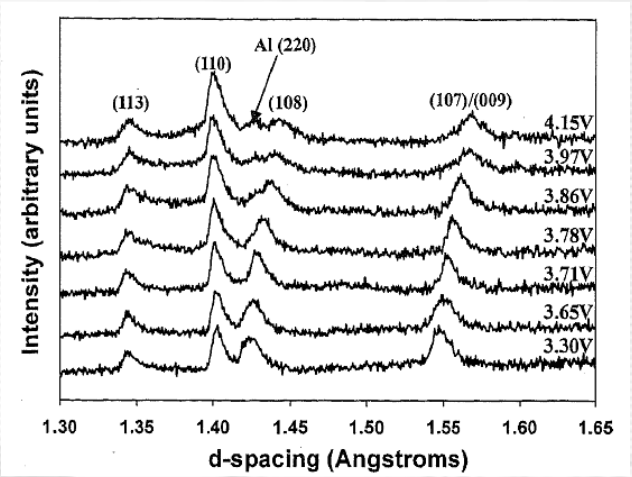

TOF neutron diffraction data as a function of voltage showing changes in *d*-spacings as cell is discharged from 4.15 to 3.30 V

Materials:

- $LiCoO_2$ type cathode
- graphite (LiC_6) anode
- Al current collector
- electrolyte (background)

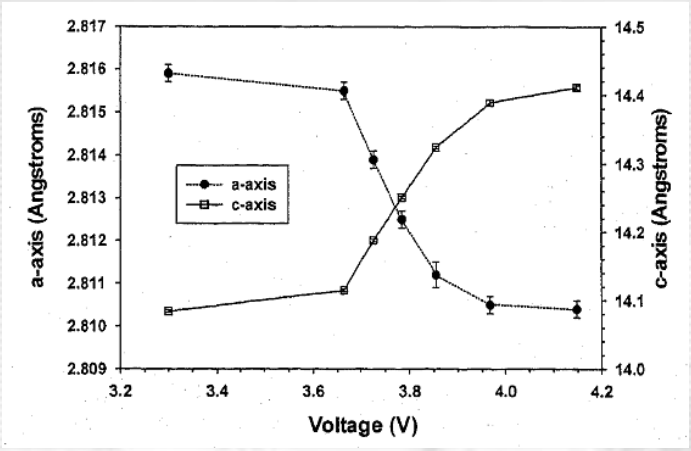

Lattice parameter for the $LiCoO_2$ type cathode as a function of the open-circuit cell voltage

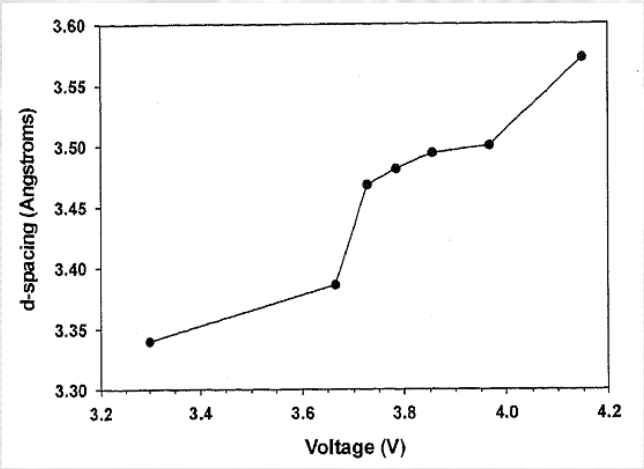

d-spacing for graphite (LiC_6) anode during a lithium-ion cell discharge displaying "staging" effects

from M.A. Rodrigues et al., Electrochem. Solid-State Letters, 2004

In Situ neutron imaging of alkaline AA cell

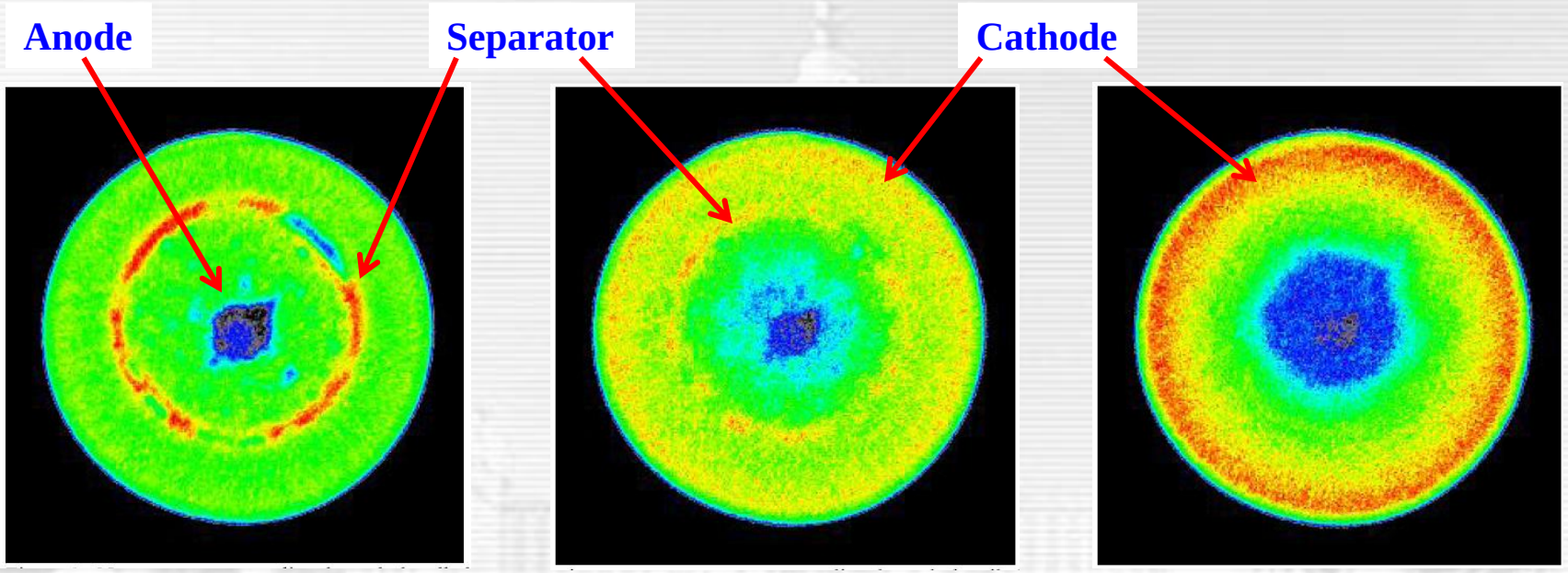

Neutron tomogram slice through the cell before discharge. The anode center post has very low neutron attenuation, while the separator (with hydrogen) has a strong attenuation.

After 17.5 h discharge at a constant current draw of 50 mA. There is increased attenuation in the cathode, indicating migration of hydrogen. The separator is still visible, although it is losing hydrogen.

After 52.5 h discharge at a constant current draw of 50 mA. There is further increased attenuation in the cathode. The separator is no longer well defined.

Daniel S. Hussey
National Institute of Standards and Technology
USA

Neutron scattering in Russia / Dubna

Research reactors in Russia

I.	JINR, Dubna, IBR-2 (1984, 2 MW) pulsed	6 Dif + 1 SANS + 2 INS + 2 Ref TOF instruments
II.	"Kurchatov Inst." Moscow, IR-8 (1957, 8 MW) steady state	2 Dif. + NI
III.	PNPI, Gatchina, VVR-M (1959, 16 MW) steady state	3 Dif. + 2 SANS + 1 INS
IV.	IMP, Yekaterinburg, IVV-2M (1966, 15 MW) steady state	4 Dif. + 1 SANS + 1 INS restricted access
V.	IPC, Obninsk, VVR-M (1960, 12 MW) steady state	2 Dif. restricted access
VI.	PNPI, Gatchina, PEAK (20??, 100 MW) steady state	under construction
VII.	NPI, Troitsk, IN-06 (20??, 100 kW) pulsed, spallation	under construction

Neutron spectrometers at the IBR-2

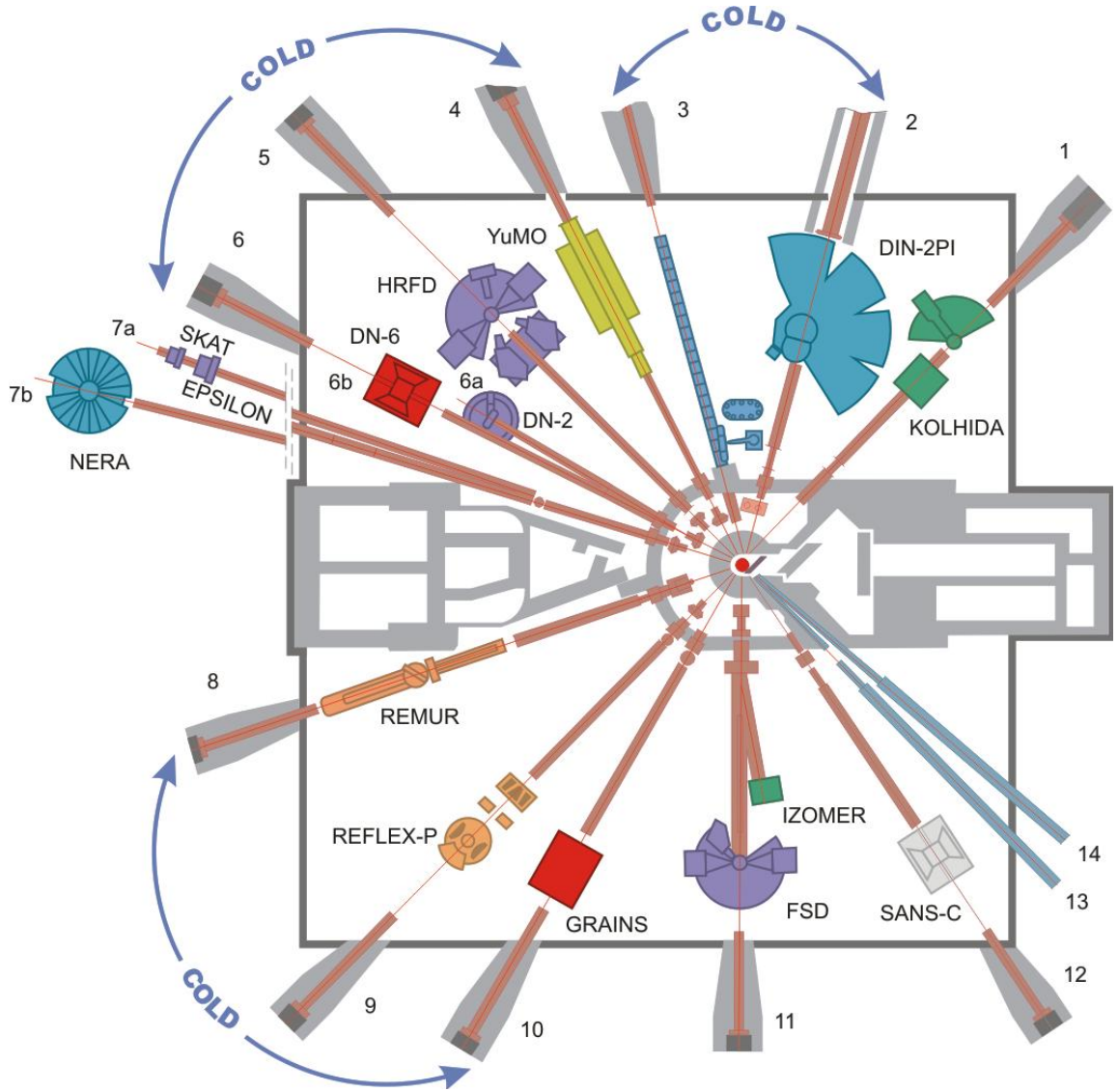

Diffraction (6):

HRFD, SKAT, EPSILON, FSD, DN-6, RTD

SANS (2):

YuMO, SANS-C

Reflectometry (3):

REMUR, REFLEX, GRAINS

Inelastic scattering (2):

NERA, DIN

13 spectrometers (4 new)

Diffraction at the IBR-2M

1. **HRFD*** **powders – *atomic and magnetic structure***
2. **FSD*** **bulk samples – *internal stresses***
3. **RTD** **powders – *real-time, in situ* (new project)**
4. **DN-6** **microsamples – *high-pressure* (new project)**
5. **EPSILON**** **rocks – *internal stresses***
6. **SKAT**** **rocks – *textures***

*** Fourier RTOF technique**

**** Long (~100 m) flight pass**

Optimization over resolution

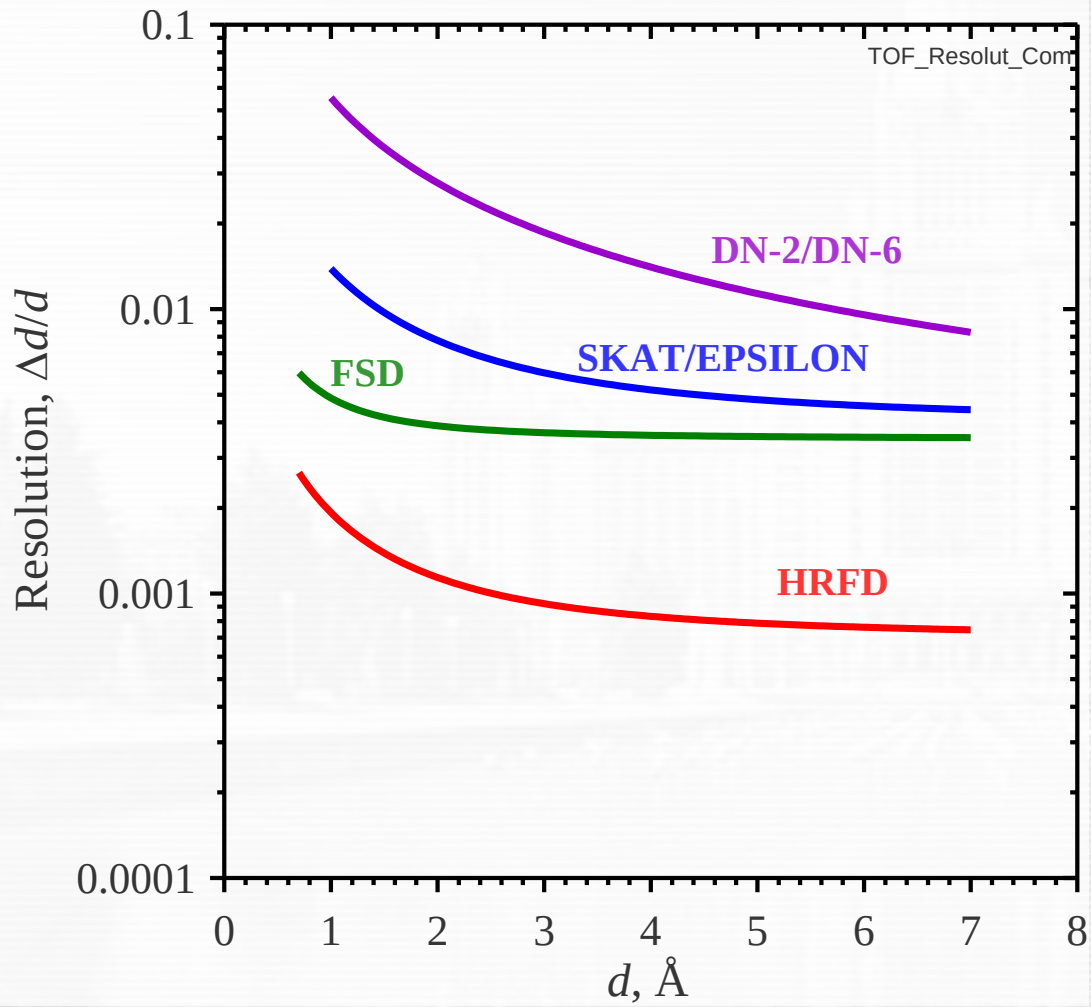

HRFD	**поликристаллы**
FSD	**напряжения**
RTD	**real-time, мембраны**
DN-6	**микрообразцы**
Epsilon	**напряжения**
SCAT	**текстуры**

Resolution becomes better for longer *d*-spacing!

Collaboration with Moscow State University

Atomic and magnetic structures of $Sr_2GaMnO_{5+\delta}$

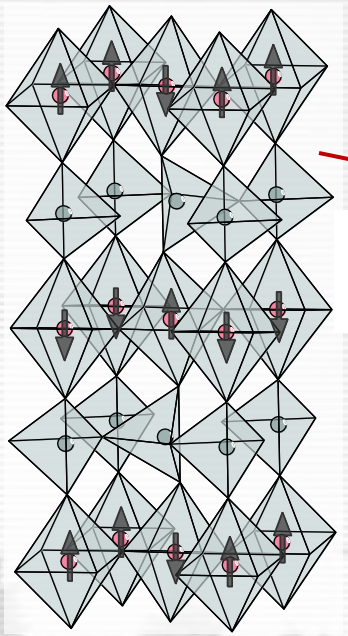

$\delta \approx 0$
AFM_G

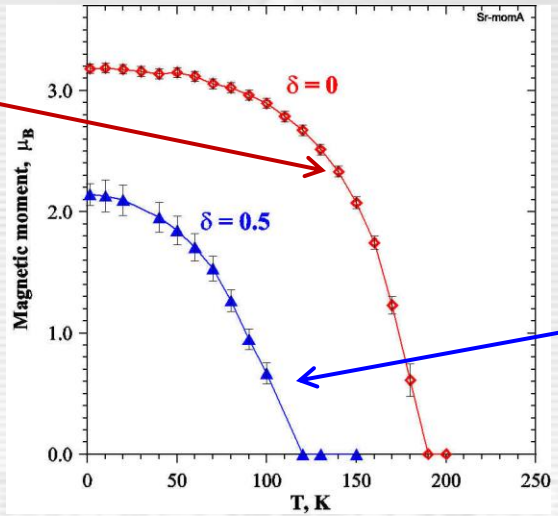

$\delta \approx 0.5$
AFM_C

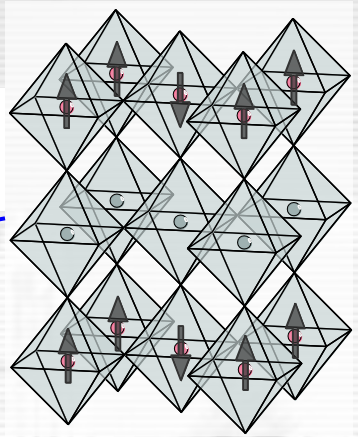

Crystal Structure of Lithium Beryllium Deuteride Li_2BeD_4

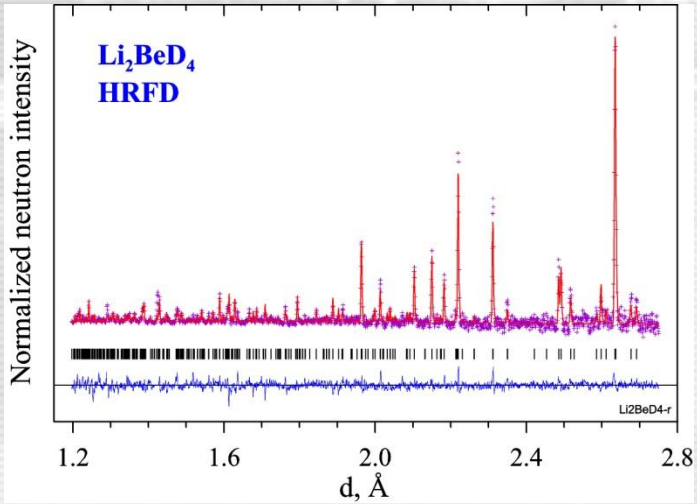

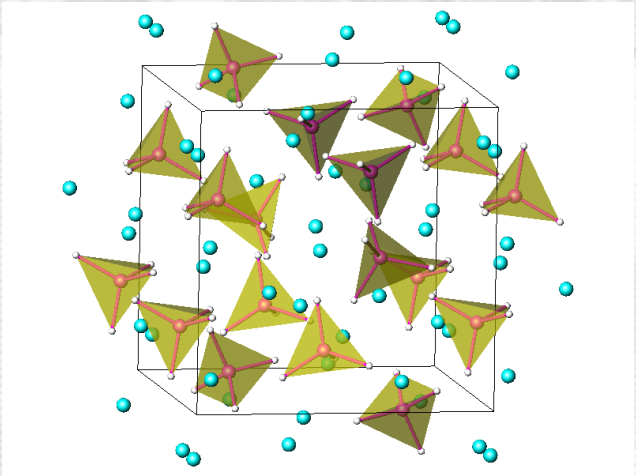

Giant oxygen isotope effect in manganites

Huge decrease of electrical resistivity under the influence of magnetic field !

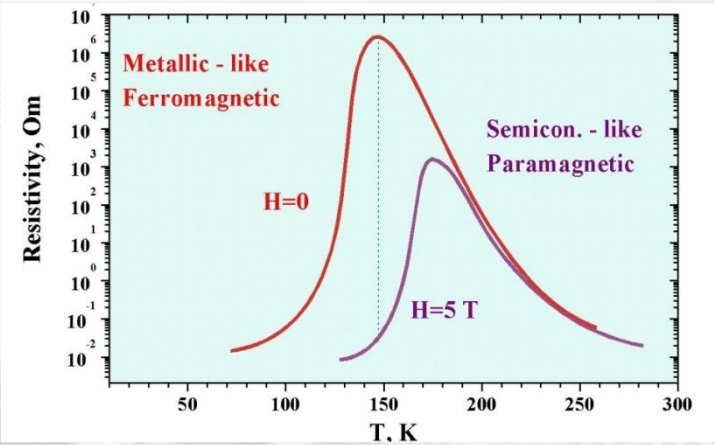

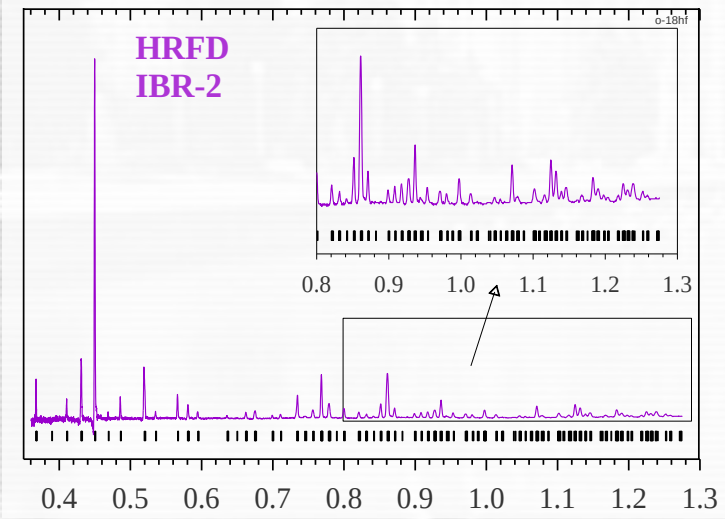

Diffraction pattern of $(La_{0.25}Pr_{0.75})_{0.7}Ca_{0.3}MnO_3$

Metal to insulator phase transition after oxygen isotope $^{16}O \rightarrow {}^{18}O$ exchange

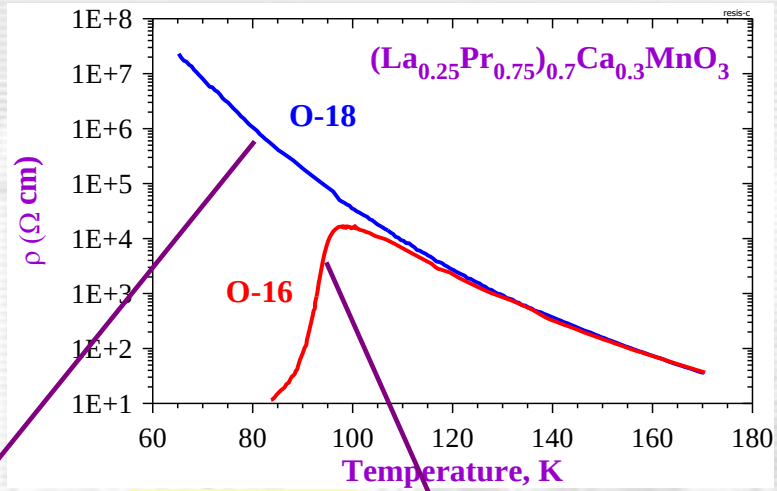

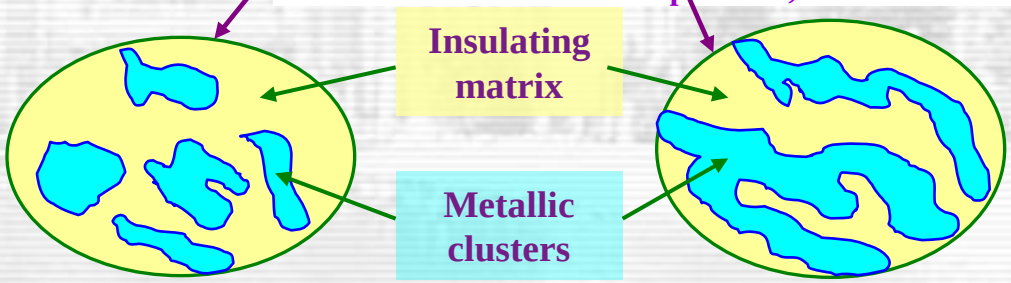

Insulating state. Separated ferromagnetic clusters

Metallic state. Infinite ferromagnetic clusters

Percolation effect in manganites

Atomic structure is different in FM and AFM phases in $(La_{0.25}Pr_{0.75})_{0.7}Ca_{0.3}MnO_3$: $^{16}O/^{18}O$

Mn-O distances

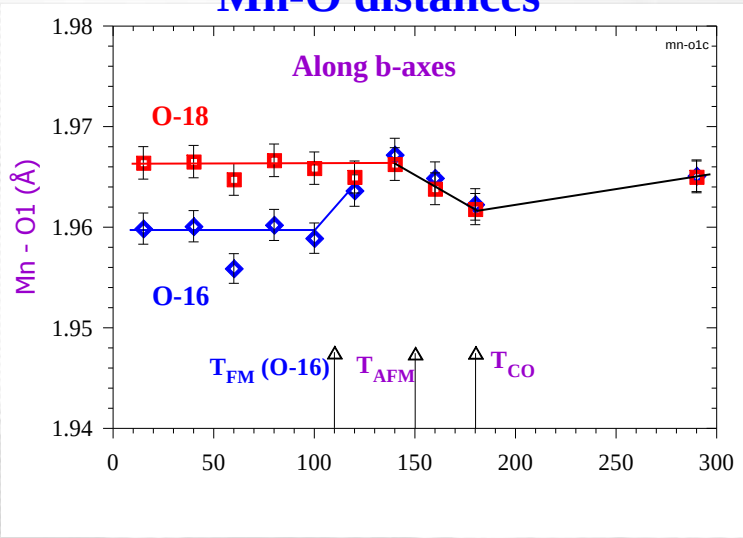

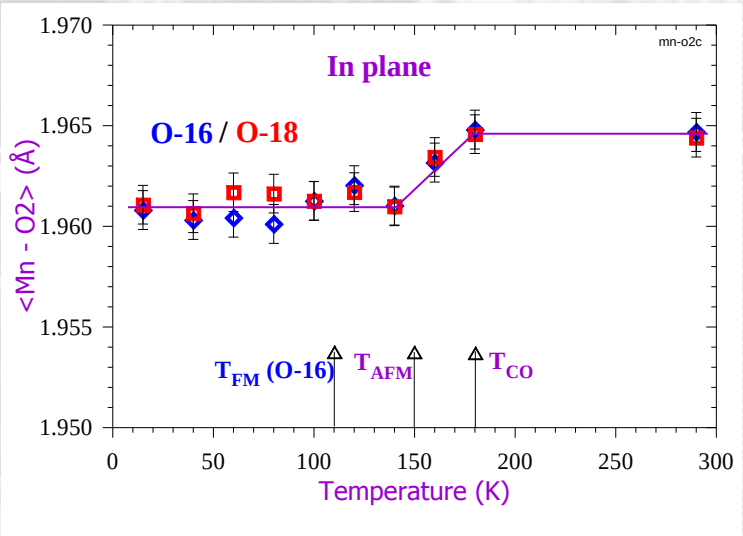

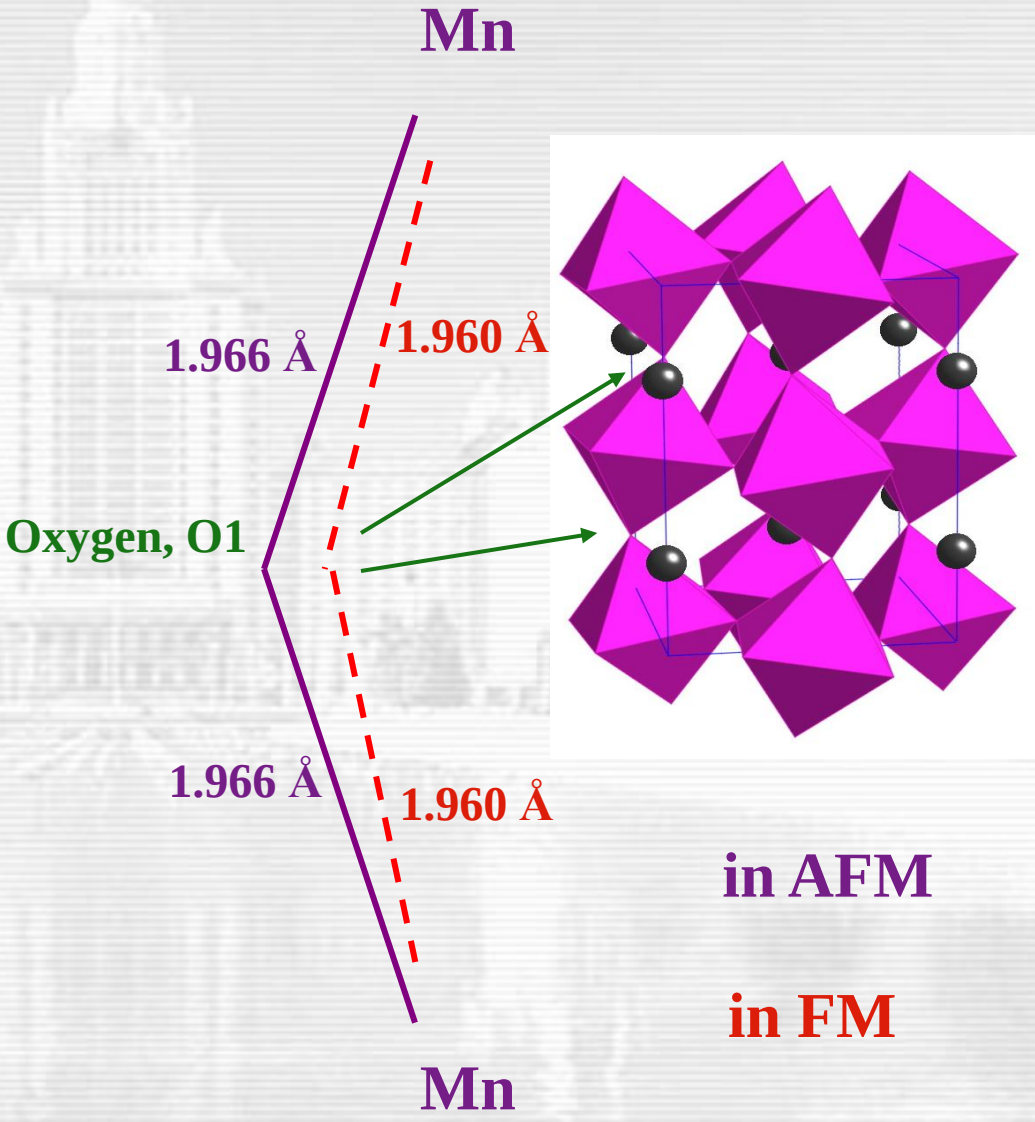

Magnetic ordering in $Sr_3YCo_4O_{10.5+\delta}$ (δ = 0.02 and 0.26)

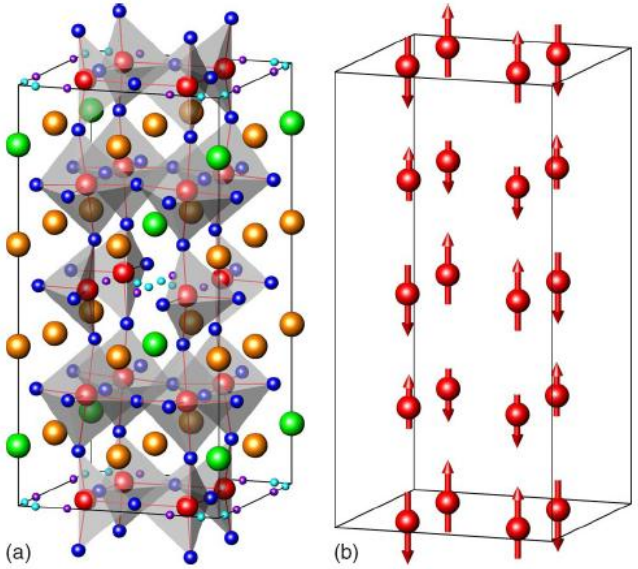

Crystal and magnetic structures of the $Sr_3YCo_4O_{10.5+\delta}$ compounds

Co1

Co2

Co1

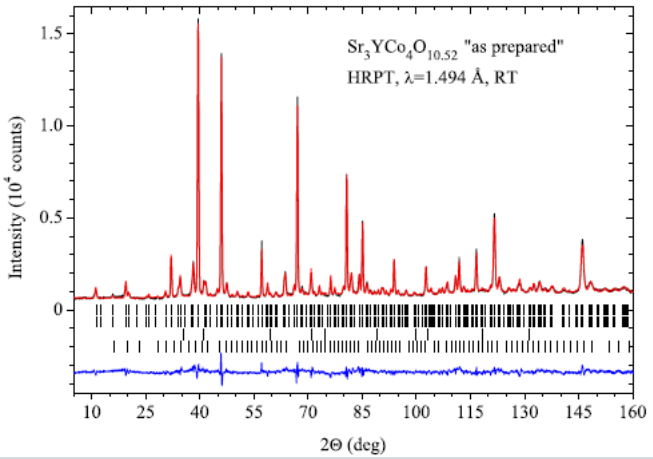

Rietveld refinement of the RT HRPT data of the $Sr_3YCo_4O_{10.52}$

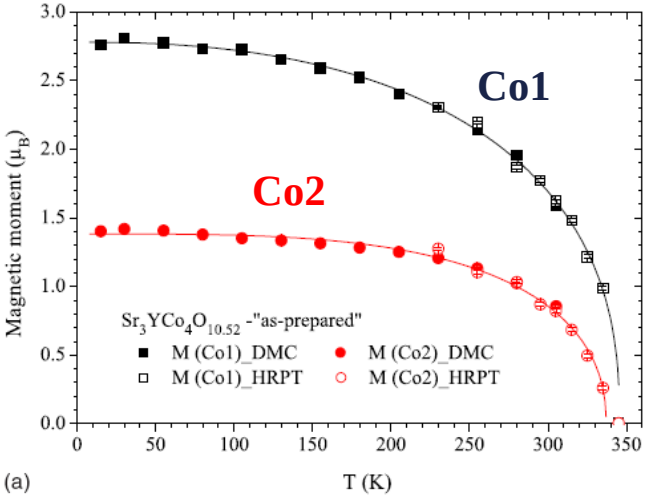

Refined magnetic moments on the Co1 and Co2 sites for the $Sr_3YCo_4O_{10.52}$ compound

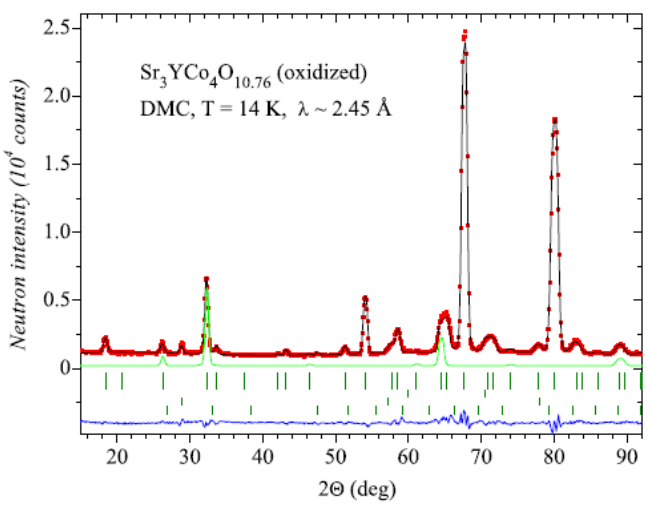

Rietveld refinement of the *T*=14 K DMC data of the $Sr_3YCo_4O_{10.76}$

Литература на русском языке

И.И.Гуревич, Л.В.Тарасов “Физика нейтронов низких энергий” М., Наука, 1965

М.П.Шаскольская “Кристаллография” М., Высшая школа, 1976

В.И.Иверонова, Г.П.Ревкевич “Теория рассеяния рентгеновских лучей” М., МГУ, 1978

Ю.З.Нозик, Р.П.Озеров, К.Хениг “Структурная нейтронография” М., Атомиздат, 1979.

Б.К.Вайнштейн “Симметрия кристаллов”, “Современная кристаллография”, т.1, М.,Наука, 1979

Г.С.Жданов, А.С.Илюшин, С.В.Никитина “Дифракционный и резонансный структурный анализ” М., Наука, 1980.

В.Л.Аксенов, А.М.Балагуров “Нейтронная дифрактометрия” УФН, т. 166 (9), с. 955, 1996.

Литература на английском языке

C.G. Windsor “Pulsed Neutron Scattering” Taylor&Francis, London, 1981

J.R.D. Copley “The Fundamentals of Neutron Powder Diffraction” NIST Special Publication, 960-2, 2001.

T. Egami, S.J.L. Billinge “Underneath the Bragg Peaks. Structural Analysis of Complex Materials” Pergamon Mat. Series, Vol. 7, Oxford, 2003.

V.K. Pecharsky, P.Y. Zavalij “Fundamentals of Powder Diffraction and Structural Characterization of Materials” Springer, 2005.

“Powder Diffraction. Theory and Practice” Ed.-s R.E. Dinnebier, S.L.J. Billinge, RSC Publishing, 2008.

A. Furrer, J. Mesot, T. Strassle “Neutron Scattering in Condensed Matter Physics” World Scientific, 2009.

Many thanks to my friends in science! Joint work with them is exciting!

Peter Fischer
Paul Scherrer Institute

Evgeny Antipov
Moscow State University

Vladimir Pomjakushin
Frank Laboratory of Neutron Physics and Paul Scherrer Institute

Denis Sheptyakov
Frank Laboratory of Neutron Physics and Paul Scherrer Institute

Thank you for attention!

Спасибо за внимание.

Желаю успехов в нелегкой, но очень интересной жизни молодого научного работника!